

Diffusive Mobile MC With Absorbing Receivers: Stochastic Analysis and Applications

Trang Ngoc Cao¹, *Student Member, IEEE*, Arman Ahmadzadeh², *Student Member, IEEE*,
 Vahid Jamali², *Member, IEEE*, Wayan Wicke³, *Student Member, IEEE*,
 Phee Lep Yeoh⁴, *Member, IEEE*, Jamie Evans⁵, *Senior Member, IEEE*,
 and Robert Schober, *Fellow, IEEE*

Abstract—This paper presents a stochastic analysis of the time-variant channel impulse response (CIR) of a three dimensional diffusive mobile molecular communication (MC) system where the transmitter, the absorbing receiver, and the molecules can freely diffuse. In our analysis, we derive the mean, variance, probability density function (PDF), and cumulative distribution function (CDF) of the CIR. We also derive the PDF and CDF of the probability p that a released molecule is absorbed at the receiver during a given time period. The obtained analytical results are employed for the design of drug delivery and MC systems with imperfect channel state information. For the first application, we exploit the mean and variance of the CIR to optimize a controlled-release drug delivery system employing a mobile drug carrier. We evaluate the performance of the proposed release design based on the PDF and CDF of the CIR. We demonstrate significant savings in the amount of released drugs compared to a constant-release scheme and reveal the necessity of accounting for the drug-carrier's mobility to ensure reliable drug delivery. For the second application, we exploit the PDF of the distance between the mobile transceivers and the CDF of p to optimize three design parameters of an MC system employing on-off keying modulation and threshold detection. Specifically, we optimize the detection threshold at the receiver, the release profile at the transmitter, and the time duration of a bit frame. We show that the proposed optimal designs can significantly improve the system performance in terms of the bit error rate and the efficiency of molecule usage.

Index Terms—Absorbing receivers, drug delivery, mobile molecular communications, stochastic channel modeling, time-varying channels.

Manuscript received August 14, 2019; revised December 13, 2019; accepted January 16, 2020. Date of publication March 9, 2020; date of current version April 20, 2020. This work was supported in part by the Diane Lemaire Scholarship of the Melbourne School of Engineering, the Australian Research Council Discovery Project under Grant DP190100770, in part by the Emerging Fields Initiative of the Friedrich–Alexander–Universität Erlangen–Nürnberg, and in part by the STAEDTLER Stiftung. This article has been presented in part at the IEEE ICC 2019 [1]. The associate editor coordinating the review of this article and approving it for publication was H. B. Yilmaz. (Corresponding author: Trang Ngoc Cao.)

Trang Ngoc Cao and Jamie Evans are with the Department of Electrical and Electronic Engineering, University of Melbourne, Melbourne, VIC 3010, Australia (e-mail: ngocc@student.unimelb.edu.au; jse@unimelb.edu.au).

Arman Ahmadzadeh, Vahid Jamali, Wayan Wicke, and Robert Schober are with the Institute for Digital Communications, Friedrich–Alexander–Universität Erlangen–Nürnberg, 91058 Erlangen, Germany (e-mail: arman.ahmadzadeh@fau.de; vahid.jamali@fau.de; wayan.wicke@fau.de; robert.schober@fau.de).

Phee Lep Yeoh is with the School of Electrical and Information Engineering, University of Sydney, Sydney, NSW 2006, Australia (e-mail: phee.yeoh@sydney.edu.au).

Digital Object Identifier 10.1109/TMBMC.2020.2979364

I. INTRODUCTION

AS APPROPRIATE channel models are essential for the analysis and design of molecular communication (MC) systems, MC channel modeling has been extensively studied in the literature [2]–[5]. For example, the simple diffusive channel model of an unbounded three-dimensional (3D) MC system with impulsive point release of information carrying molecules [3] has been widely used for system analysis and design [4], [5]. Diffusion channel models with drift [6] and chemical reactions [7] have also been considered. However, most of the previously studied MC channel models assume static communication systems where the transceivers do not move.

Recently, in addition to applications with static transceivers, e.g., sensors monitoring the environment [3] and communication in water pipes and underground environments [4], many applications have emerged where the transceivers are mobile, including drug delivery [8], mobile ad hoc nanonetworks [9], and detection of mobile targets [10]. Hence, the modeling and design of mobile MC systems have gained considerable attention, see [2], [9]–[16]. In [9], a mobile ad hoc nanonetwork was considered where mobile nanomachines collect environmental information and deliver it to a mobile central control unit. The mobility of the nanomachines was described by a 3D model but information was only exchanged when two nanomachines collided. In [10], a leader-follower-based model for two-dimensional mobile MC networks for target detection with non-diffusive information molecules was proposed. The authors in [11] considered adaptive detection and inter-symbol interference (ISI) mitigation in mobile MC systems, while [12] analyzed the mutual information and maximum achievable rate in such systems. However, the authors of [11] and [12] did not provide a stochastic analysis of the time-variant channel but analyzed the system numerically. In [13], a comprehensive framework for modeling the time-variant channels of diffusive mobile MC systems with diffusive transceivers was developed. However, all of the works mentioned above assumed a passive receiver.

On the other hand, for many MC applications, a fully absorbing receiver is considered to be a more realistic model compared to a passive receiver as it captures the interaction between the receiver and the information molecules, e.g., the conversion of the information molecules to a new type of

molecule or the absorption and removal of the information molecules from the environment [3], [4]. Since the molecules are removed from the environment after being absorbed by the receiver, the channel impulse response (CIR) for absorbing receivers is a more complicated function of the distance between the transceivers and the receiver's radius compared to passive receivers. Therefore, the stochastic analysis of mobile MC systems with absorbing receivers is very challenging. For the fully absorbing receiver in diffusive mobile MC systems, theoretical expressions for the average distribution of the first hitting time, i.e., the mean of the CIR, were derived for a *one-dimensional (1D)* environment without drift in [14] and with drift in [15]. Based on the 1D model in [14], the error rate and channel capacity of the system were examined in [16]. However, none of these works provides a statistical analysis of the time-variant CIR of a 3D diffusive mobile MC system with absorbing receiver. In this paper, we address this issue and exploit the obtained analytical results for the stochastic parameters of the time-variant MC channel for the design of drug delivery and MC systems. The stochastic analysis for the absorbing receiver presented in this work is much more challenging than the analysis for the passive receiver presented in [13]. Furthermore, the application of stochastic analysis to the design of drug delivery and MC systems was not considered in [13].

In drug delivery systems, drug molecules are carried to diseased cell sites by nanoparticle drug carriers, so that the drug is delivered to the targeted site without affecting healthy cells [8]. After being injected or extravasated from the cardiovascular system into the tissue surrounding a targeted diseased cell site, the drug carriers may not be anchored at the targeted site but may move, mostly via diffusion [17]–[20]. The diffusion of the drug carriers results in a time-variant absorption rate of the drugs even if the drug release rate is constant. Furthermore, experimental and theoretical studies have indicated that the total drug dosage as well as the rate and time period of drug absorption by the receptors of the diseased cells are critical factors in the healing process [19], [21]. Therefore, to reduce drug cost, over-dosing, and negative side effects to healthy cells yet satisfy the treatment requirements, it is important to optimize the release profile of drug delivery systems such that the total amount of released drugs is minimized while a desired rate of drug absorption at the diseased site during a prescribed time period is achieved. To this end, the mobility of the drug carriers and the absorption rate of the drugs have to be accurately taken into account. This can be accomplished by exploiting the MC paradigm where the drug carriers, diseased cells, and drug molecules are modeled as mobile transmitters, absorbing receivers, and signaling molecules, respectively [4]. Release profile designs for drug delivery systems based on an MC framework were proposed in [5], [22]–[24]. However, in these works, the transceivers were fixed and only the movement of the drug molecules was considered. In this paper, we exploit the analytical results obtained for the stochastic parameters of the time-variant MC channel with absorbing receiver for the optimization of the release profile of drug delivery systems with mobile drug carriers.

In diffusive mobile MC systems, knowledge of the CIR is needed for reliable communication design. However, the CIR may not always be available in a diffusive mobile MC system due to the random movements of the transceivers. In particular, the distance between the transceivers at the time of release, on which the CIR depends, may only be known at the start of a transmission frame. In other words, the movement of the transceivers causes the CSI to become outdated, which makes communication system design challenging. In this paper, we consider a mobile MC system employing on-off keying and threshold detection and optimize three design parameters to improve the system performance under imperfect CSI. First, we optimize the detection threshold at the receiver for minimization of the maximum bit error rate (BER) in a frame when the number of molecules available for transmission is uniformly allocated to each bit of the frame. Second, we optimize the release profile at the transmitter, i.e., the optimal number of molecules available for the transmission of each bit, for minimization of the maximum BER in a frame given a fixed number of molecules available for transmission of the entire frame. Third, we maximize the frame duration under the constraint that the probability that a released molecule is absorbed by the receiver does not fall below a prescribed value. Such a design ensures that molecules are used efficiently as a molecule release occurs only if the released molecule is observed at the receiver with sufficiently high probability. For the proposed design tasks, the results for the stochastic analysis of the transceivers' positions and for the probability that a molecule is absorbed during a given time period are exploited.

The main contributions of this paper can be summarized as follows:

- We provide a statistical analysis of the time-variant channel of a 3D diffusive mobile MC system employing an absorbing receiver. In particular, we derive the mean, variance, PDF, and CDF of the corresponding CIR. Moreover, we derive the PDF and CDF of the probability that a molecule is absorbed during a given time period. The stochastic channel analysis is exploited for the offline design of drug delivery and MC systems.
- For drug delivery systems, we propose a framework for optimization of the release profile for minimization of the amount of released drugs while ensuring that the absorption rate at the diseased cells does not fall below a prescribed threshold for a given period of time. We show that the optimal release profile can be divided into three phases and that the proposed design requires a significantly lower amount of released drugs compared to a design with a constant release rate. We also propose and derive a metric for evaluation of the system performance, namely the probability that the drug absorption rate satisfies the target rate.
- For MC systems employing on-off keying modulation and threshold detection based on imperfect CSI, we optimize three design parameters, namely the detection threshold at the receiver, the release profile at the transmitter, and the time duration of a bit frame. To this end, for simplicity of system design, we assume that the symbol interval

is large enough such that ISI is not significant. ISI can be efficiently reduced by introducing chemical reactions in the environment [7], [25], [26]. Our results show that, for MC systems, the optimal release profile is increasing over the frame duration. Moreover, we show that the proposed designs enable significant performance gains in terms of the BER and the efficiency of molecule usage compared to baseline systems with uniform molecule release and without limitation on time duration of a bit frame, respectively.

- Our results reveal that the transceivers' mobility has a significant impact on the system performance and should be carefully taken into account for MC system design.

We note that the derived analytical results for the time-variant CIR of mobile MC systems with absorbing receiver are expected to be useful not only for the design of the drug delivery and MC systems considered in this paper but also for the design of detection schemes and the evaluation of the performance (e.g., the capacity and throughput) of such systems.

This paper expands its conference version [1]. In particular, the analysis of the probability that a molecule is absorbed during a given time period, the MC system design for imperfect CSI, and the corresponding simulation results are not included in [1].

The remainder of this paper is organized as follows. In Section II, we introduce the considered diffusive mobile MC system with absorbing receiver and the time-variant channel model. In Section III, we provide the proposed statistical analysis of the time-variant channel. In Sections IV and V, we apply the derived results for optimization of drug delivery and MC systems with imperfect CSI, respectively. Numerical results are presented in Section VI, and Section VII concludes the paper.

II. GENERAL SYSTEM AND CHANNEL MODEL

In this section, we first introduce the model for a general diffusive mobile MC system with absorbing receiver. Subsequently, we specialize the model to drug delivery and communication systems with imperfect CSI. Finally, we define the time-variant CIR and the received signal.

A. System Model

We consider a linear diffusive mobile MC system in an unbounded 3D environment with constant temperature and viscosity. The system comprises one mobile spherical transparent transmitter, denoted by Tx, with radius a_{Tx} , one mobile spherical absorbing receiver, denoted by Rx, with radius a_{Rx} , and the signaling molecules of type X.

The movements of the Tx, Rx, and X molecules are assumed to be mutually independent and to follow Brownian motion with diffusion coefficients D_{Tx} , D_{Rx} , and D_X , respectively. This assumption, which was also made in [13] and [14], is motivated by the fact that the mobility of small objects is governed by Brownian motion.

We assume that Tx releases molecules at its center instantaneously and discretely during the considered period of time

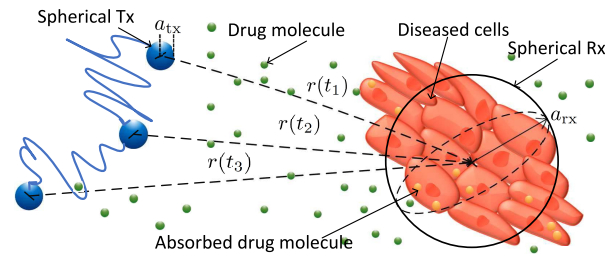


Fig. 1. System model for drug delivery. The drug carrier and the diseased cells of a tumor are modeled as diffusive spherical transmitter (Tx) and spherical absorbing receiver (Rx), respectively. The drug molecules are absorbed by Rx, when they hit its surface. Different distances between Tx and Rx over time are due to Tx's diffusion.

denoted by T . Let t_i and T_b denote the time instant of the i -th release and the duration of the interval between the i -th and the $(i+1)$ -th release, respectively. We have $t_i = (i-1)T_b$ and $i \in \{1, \dots, I\}$, where I is the total number of releases during T . We denote the time-varying distance between the centers of Tx and Rx at time t by $r(t)$. Furthermore, let α_i and $A = \sum_{i=1}^I \alpha_i$ denote the number of molecules released at time t_i and the total number of molecules released during T , respectively. For concreteness, we specialize the considered general model to two application scenarios.

1) *Drug Delivery Systems*: A drug delivery system comprises a drug carrier releasing drug molecules and diseased cells absorbing them. We model the drug carrier and diseased cells as Tx and Rx of the general MC system, respectively, see Fig. 1. The drug carriers in drug delivery systems are typically nanoparticles, such as spherical polymers or polymer chains, having a size not smaller than 100 nm [18]. Moreover, drug carriers are designed to carry drug molecules and interaction with the drug or the receiver is not intended. Hence, the drug carriers can be modeled as mobile spherical transparent transmitters, Tx. When the drug molecules hit the tumor, they are absorbed by receptors on the surface of the diseased cells [19], [21]. For convenience, we model the tumor as a spherical absorbing receiver, Rx. In reality, the colony of cancer cells may potentially have a different geometry, of course. However, as an abstract approximation, we model the cancer cells as one effective spherical receiver with radius a_{Rx} and with a surface area equivalent to the total surface area of the tumor (see Fig. 1). Hence, the absorptions on the actual and the modeled surfaces are expected to be comparable [17].

In a drug delivery system, the drug carriers can be directly injected or extravasated from the blood into the interstitial tissue near the diseased cells, where they start to move.¹ We assume that the injection position can be estimated and thus $r(t=0)$ is known. The movement of the drug carrying nanoparticles in the tissue is caused by diffusion and convection mechanisms but diffusion is expected to be dominant near the tumor site in most cases [17]–[20]. This is because

¹If the drug carriers are not injected near the tumor, modeling their delivery to the diseased area is challenging due to the involved multi-scale channel where the molecules first have to travel a macro-scale distance to reach the target area and then enter the capillaries whose size is at micro-scale. We leave the consideration of this multi-scale problem for future work and focus here on the micro-scale delivery of the drug molecules, where the drug carriers have arrived near the tumor, e.g., by direct injection or via the capillaries.

the abnormal physiology of tumors causes outward interstitial pressure which counteracts the inward convective flow and thus leaves diffusion as the main transport mechanism near tumors [17], [20]. At the tumor site, the drug carrier releases drug molecules of type X, which also diffuse in the tissue [19]. Hence, we can adopt Brownian motion to model the diffusion of Tx and X molecules with diffusion coefficients D_{Tx} , and D_X , respectively [8]. We consider a rooted tumor and thus $D_{Rx} = 0$, which is a special case of the considered general system model.

We assume the instantaneous and discrete release of drugs. After releasing for a period of time, the drug carrier may be removed by blood circulation or run out of drugs. Thus, for drug delivery systems, T , T_b , t_i , and I denote the release period of the drug, the duration of the interval between two releases, the release instants of the drug molecules, and the number of releases, respectively. A continuous release can be approximated by letting $T_b \rightarrow 0$, i.e., $I \rightarrow \infty$. Moreover, A and α_i denote the total number of drug molecules released during T and the number of drug molecules released at time t_i , respectively.

2) *Molecular Communication System*: For the considered MC system, we assume Brownian motion of the transceivers and signaling molecules. We assume multi-frame communication between mobile Tx and Rx with instantaneous molecule release for each bit transmission. Hence, T , T_b , t_i , and I denote the duration of a bit frame, the duration of one bit interval, the beginning of the i -th bit interval, and the number of bits in a frame, respectively. For an arbitrary bit frame, let b_i , $i \in \{1, \dots, I\}$, denote the i -th bit in the bit frame. We assume that symbols 0 and 1 are transmitted independently and with equal probability. Thus, the probability of transmitting \tilde{b}_i is $\Pr(\tilde{b}_i) = 1/2$, where $\Pr(\cdot)$ denotes probability and $\tilde{b}_i \in \{0, 1\}$ is a realization of b_i . We assume that on-off keying modulation is employed. At time t_i , Tx releases α_i molecules to transmit bit 1 and no molecules for bit 0. Then, $A = \sum_{i=1}^I \alpha_i$ is the total number of molecules available for transmission in a given bit frame.

B. Time-Variant CIR and Received Signal

Considering again the general system model, we now model the channel between Tx and Rx as well as the received signals at Rx for drug delivery and MC systems, respectively.

1) *Time-Variant CIR*: Let $h(t, \tau)$ denote the hitting rate, i.e., the absorption rate of a given molecule, at time τ after its release at time t at the center of Tx. Then, for an infinitesimally small observation window $\Delta\tau$, i.e., $\Delta\tau \rightarrow 0$, we can interpret $h(t, \tau)\Delta\tau$ as the probability of absorption of a molecule by Rx between times τ and $\tau + \Delta\tau$ after its release at time t . The hitting rate $h(t, \tau)$ is also referred to as the CIR since it completely characterizes the time-variant channel, which is assumed to be linear.

For a given distance between Tx and Rx, $r(t)$, the CIR $h(t, \tau)$ of a diffusive mobile MC system at time τ is given by [2], [3]

$$h(t, \tau) = \frac{a_{rx}}{\sqrt{4\pi D_1 \tau^3}} \left(1 - \frac{a_{rx}}{r(t)}\right) \exp\left(-\frac{(r(t) - a_{rx})^2}{4D_1 \tau}\right), \quad (1)$$

for $\tau > 0$ and $h(t, \tau) = 0$, for $\tau \leq 0$. Here, D_1 is the effective diffusion coefficient capturing the relative motion of the signaling molecules and Rx. Since the signaling molecules diffuse with diffusion coefficient D_X and Rx diffuses with diffusion coefficient D_{Rx} , the combined movement of the signaling molecules and Rx is characterized by diffusion coefficient $D_1 = D_X + D_{Rx}$, see [27, eq. (8)] for details. In the considered MC system, due to the motion of the transceivers, the distance $r(t)$ is a random variable, and thus, the CIR $h(t, \tau)$ is time-variant and should be modeled as a stochastic process [13].

2) *Received Signal for Drug Delivery System*: In drug delivery, the absorption rate ultimately determines the therapeutic impact of the drug [19], [21]. Thus, we formally define the absorption rate as the desired received signal, and make achieving a desired absorption rate the objective for system design. Recall that $h(t, \tau)\Delta\tau$, $\Delta\tau \rightarrow 0$, is the probability of absorption of a molecule by Rx between times τ and $\tau + \Delta\tau$ after the release at time t . If α_i molecules are released at Tx at time t_i , the expected number of molecules absorbed at Rx between times t and $t + \Delta t$, for $\Delta t \rightarrow 0$, due to this release is $\alpha_i h(t_i, t - t_i)\Delta t$. During the period $[0, t]$, the total number of released drug molecules is $A_t = \sum_i \alpha_i$, $\forall i | t_i < t$, and the expected number of drug molecules absorbed between times t and $t + \Delta t$, for $\Delta t \rightarrow 0$ is given by $s(t) = \sum_i \alpha_i h(t_i, t - t_i)\Delta t$, $\forall i | t_i < t$. Let $g(t)$ denote the absorption rate of drug molecules X at Rx at time t , i.e., $g(t) = s(t)/\Delta t$, $\Delta t \rightarrow 0$. Then, we have

$$g(t) = \sum_{\forall i | t_i < t} \alpha_i h(t_i, t - t_i). \quad (2)$$

As mentioned before, the absorption rate $g(t)$, i.e., the received signal, of the tumor cells directly affects the healing efficacy of the drug. Hence, we will design the drug delivery system such that $g(t)$ does not fall below a prescribed value. Since $g(t)$ is a function of $h(t_i, t - t_i)$, it is random due to the diffusion of Tx. Therefore, the design of the drug delivery system has to take into account the statistical properties of $g(t)$, which can be obtained from the results of the statistical analysis of $h(t_i, t - t_i)$.

3) *Received Signal for MC System*: For the MC system design, the received signal, denoted by q_i , is defined as the number of X molecules absorbed at Rx during bit interval T_b after the transmission of the i -th bit at t_i by Tx as the received signal, denoted by q_i . We detect the transmitted information based on the received signal, q_i . It has been shown in [7] that q_i follows a Binomial distribution that can be accurately approximated by a Gaussian distribution when α_i is large, which we assume here. We focus on the effect of the transceivers' movements on the MC system performance and design the optimal release profile of Tx to account for these movements. We assume the bit interval to be sufficiently long such that most of the molecules have been captured by or have moved far away from Rx before the following bit is transmitted, i.e., ISI is negligible. For shorter symbol intervals, enzymes [7] and reactive information molecules, such as acid/base molecules [25], [26], may be used to speed up the molecule removal process and to increase the accuracy

of the ISI-free assumption. When ISI is not negligible, the BER will be higher than the BER expected based on the analysis and design developed in this paper. Moreover, we model external noise sources in the environment as Gaussian background noise with mean and variance equal to η [2]. Thus, we have

$$q_i \sim \mathcal{N}\left(\mu_{i,\tilde{b}_i}, \sigma_{i,\tilde{b}_i}^2\right) \text{ for } b_i = \tilde{b}_i, \quad (3)$$

where $\mu_{i,0} = \sigma_{i,0}^2 = \eta$, $\mu_{i,1} = \alpha_i p(t_i, T_b) + \eta$, $\sigma_{i,1}^2 = \alpha_i p(t_i, T_b)(1 - p(t_i, T_b)) + \eta$. Here, $\mathcal{N}(\mu, \sigma^2)$ denotes a Gaussian distribution with mean μ and variance σ^2 . $p(t, T_b)$ denotes the probability that a signaling molecule is absorbed during bit interval T_b after its release at time t at the center of Tx. For a given distance $r(t)$, $p(t, T_b)$ is given by [3]

$$p(t, T_b) = \int_0^{T_b} h(t, \tau) d\tau = \frac{a_{\text{rx}}}{r(t)} \operatorname{erfc}\left(\frac{r(t) - a_{\text{rx}}}{2\sqrt{D_1 T_b}}\right), \quad (4)$$

where $\operatorname{erfc}(\cdot)$ is the complementary error function. Since $r(t)$ is a random variable and $p(t, T_b)$ is a function of $r(t)$, $p(t, T_b)$ and any function of $p(t, T_b)$, e.g., the received signal q_i , are random processes. Moreover, $p(t, T_b)$ is also a function of $h(t, \tau)$. Hence, for MC system design, we have to take into account the statistical properties of $p(t, T_b)$, which can be obtained based on the proposed statistical analysis of $r(t)$ and $h(t, \tau)$.

In summary, the design of both drug delivery and MC systems depends on the statistical properties of the CIR, $h(t, \tau)$, and $r(t)$ including their means, variances, PDFs, and CDFs, which will be analyzed in the next section.

III. STOCHASTIC CHANNEL ANALYSIS

In this section, we first analyze the distribution of the distance between the transceivers, $r(t)$, and then use it to derive the statistics of the time-variant CIR, $h(t, \tau)$, and $p(t, T_b)$ as a function $h(t, \tau)$. In particular, we develop analytical expressions for the mean, variance, PDF, and CDF of $h(t, \tau)$ and the PDF and CDF of $p(t, T_b)$.

A. Distribution of the Tx-Rx Distance for a Diffusive System

In the 3D space, $r(t)$ is given by $r(t) = \sqrt{\sum_{d \in \{x,y,z\}} (r_{d,\text{Rx}}(t) - r_{d,\text{Tx}}(t))^2}$, where $r_{d,\text{Tx}}(t)$ and $r_{d,\text{Rx}}(t)$, $d \in \{x,y,z\}$, are the Cartesian coordinates representing the positions of Tx and Rx at time t , respectively. Let us assume, without loss of generality, that the diffusion of Tx and Rx starts at $t = 0$. Then, given the Brownian motion model for the mobility of Tx and Rx, we have $r_{d,\text{Tx}}(t) \sim \mathcal{N}(r_{d,\text{Tx}}(t=0), 2D_{\text{Tx}}t)$ and $r_{d,\text{Rx}}(t) \sim \mathcal{N}(r_{d,\text{Rx}}(t=0), 2D_{\text{Rx}}t)$, where we assume that $r_{d,\text{Tx}}(t=0)$ and $r_{d,\text{Rx}}(t=0)$ are known. Let us define $r_d(t) = r_{d,\text{Rx}}(t) - r_{d,\text{Tx}}(t)$. Then, we have $r_d(t) \sim \mathcal{N}(r_d(t=0), 2D_2t)$, where $D_2 = D_{\text{Tx}} + D_{\text{Rx}}$ is the effective diffusion coefficient capturing the relative motion of Tx and Rx, see [27, eq. (10)]. Given the Gaussian distribution of $r_d(t)$, we know that [28]

$$\gamma = \frac{r(t)}{\sqrt{2D_2t}} = \sqrt{\frac{\sum_{d \in \{x,y,z\}} r_d^2(t)}{2D_2t}} \quad (5)$$

follows a noncentral chi-distribution, i.e., $\gamma \sim \mathcal{X}_k(\lambda)$, with $k = 3$ degrees of freedom and parameter $\lambda = \sqrt{\frac{\sum_{d \in \{x,y,z\}} r_d^2(t=0)}{2D_2t}} = \frac{r_0}{\sqrt{2D_2t}}$, where r_0 denotes $r(t=0)$. The statistical properties of random variable $r(t)$ are provided in the following lemma.

Lemma 1: The mean, variance, PDF, and CDF of random variable $r(t)$, which represents the distance between the centers of the diffusive mobile Tx and Rx, are given by, respectively,

$$\begin{aligned} \mathbb{E}\{r(t)\} &= \sqrt{\frac{4D_2t}{\pi}} \exp\left(-\frac{r_0^2}{4D_2t}\right) \\ &\quad + \left(r_0 + \frac{2D_2t}{r_0}\right) \operatorname{erf}\left(\frac{r_0}{\sqrt{4D_2t}}\right), \end{aligned} \quad (6)$$

$$\operatorname{Var}\{r(t)\} = r_0^2 + 6D_2t - \mathbb{E}^2\{r(t)\}, \quad (7)$$

$$f_{r(t)}(r) = \frac{r}{r_0\sqrt{\pi D_2t}} \exp\left(-\frac{r^2 + r_0^2}{4D_2t}\right) \sinh\left(\frac{r_0 r}{2D_2t}\right), \quad (8)$$

and

$$F_{r(t)}(r) = 1 - \mathbf{Q}_{\frac{3}{2}}\left(\lambda, \frac{r}{\sqrt{2D_{\text{Tx}}t}}\right), \quad (9)$$

where $\operatorname{erf}(\cdot)$ is the error function, $\mathbf{Q}_M(a, b)$ is the Marcum Q-function [29], $\mathbb{E}\{\cdot\}$ denotes statistical expectation, $\operatorname{Var}\{\cdot\}$ denotes variance, and $f_{\{\cdot\}}(\cdot)$ and $F_{\{\cdot\}}(\cdot)$ denote the PDF and CDF of the random variable in the subscript, respectively.

Proof: Please refer to Appendix A. ■

Remark 1: From (6) and (7), we can observe that when $t \rightarrow \infty$, we have $\exp(-\frac{r_0^2}{4D_2t}) \rightarrow 1$ and $\operatorname{erf}(\frac{r_0}{\sqrt{4D_2t}}) \rightarrow 0$ and, as a result, $\mathbb{E}\{r(t)\} \rightarrow \infty$. Intuitively, because of diffusion, the transceivers eventually move far away from each other on average.

Remark 2: We note that (8) was derived under the assumption that Tx can diffuse in the entire 3D environment. However, in reality, Tx cannot move inside Rx, i.e., it does not interact with Rx, and thus will be reflected when it hits Rx's boundary. Hence, the actual $f_{r(t)}(r)$, derived in [27], differs from (8), e.g., $f_{r(t)}(r) = 0$ for $r < a_{\text{tx}} + a_{\text{rx}}$. However, for very small r , i.e., $r \approx 0$, (8) approaches zero. Hence, (8) is a valid approximation for the actual $f_{r(t)}(r)$. The validity of this approximation is evaluated in Section VI via simulations, where, in our particle-based simulation, Tx is reflected upon collision with Rx [30].

B. Statistical Moments of Time-Variant CIR

In this subsection, we derive the statistical moments of the time-variant CIR, i.e., mean $m(t, \tau)$ and variance $\sigma^2(t, \tau)$. In particular, the mean of the time-variant CIR, $m(t, \tau)$, can be written as

$$m(t, \tau) = \int_0^\infty h(t, \tau) \Big|_{r(t)=r} f_{r(t)}(r) dr. \quad (10)$$

A closed-form expression for (10) is provided in the following theorem.

Theorem 1: The mean of the impulse response of a time-variant channel with diffusive molecules released by a diffusive transparent transmitter and captured by a diffusive

absorbing receiver is given by

$$\begin{aligned}
m(t, \tau) &= \frac{a_{\text{rx}}}{4\sqrt{\pi}(D_1\tau + D_2t)r_0\tau} \exp\left(-\frac{a_{\text{rx}}^2}{4D_1\tau} - \frac{r_0^2}{4D_2t}\right) \\
&\left[-e^{\frac{v(t, \tau)^2}{4u(t, \tau)}} \left(\frac{v(t, \tau)}{2u(t, \tau)} + a_{\text{rx}} \right) \operatorname{erfc}\left(\frac{v(t, \tau)}{2\sqrt{u(t, \tau)}}\right) \right. \\
&\quad \left. + e^{\frac{w(t, \tau)^2}{4u(t, \tau)}} \left(\frac{w(t, \tau)}{2u(t, \tau)} + a_{\text{rx}} \right) \operatorname{erfc}\left(\frac{w(t, \tau)}{2\sqrt{u(t, \tau)}}\right) \right], \quad (11)
\end{aligned}$$

where $u(t, \tau)$, $v(t, \tau)$, and $w(t, \tau)$ are defined, for compactness, as follows

$$\begin{aligned}
u(t, \tau) &= \frac{1}{4D_1\tau} + \frac{1}{4D_2t}, \\
v(t, \tau) &= -\frac{a_{\text{rx}}}{2D_1\tau} - \frac{r_0}{2D_2t}, \\
w(t, \tau) &= -\frac{a_{\text{rx}}}{2D_1\tau} + \frac{r_0}{2D_2t}. \quad (12)
\end{aligned}$$

Proof: Substituting (1) and (8) into (10) and using the integrals given by [31, eq. (2.3.15.4) and eq. (2.3.15.7)], we obtain the expression for $m(t, \tau)$ in (11). ■

Remark 3: $m(t, \tau)$ is a function of time t . Hence, $h(t, \tau)$ is a non-stationary stochastic process. In general, at large t , $m(t, \tau)$ decreases when t increases and eventually approaches zero when $t \rightarrow \infty$. This means that as t increases, the molecules released by Tx, on average, have a decreasing chance of being absorbed by Rx since the transceivers move away from each other as mentioned in Remark 1.

In order to obtain the variance of $h(t, \tau)$,

$$\sigma^2(t, \tau) = \phi(t, \tau) - m^2(t, \tau), \quad (13)$$

we first need to find an expression for the second moment $\phi(t, \tau)$, defined as $\phi(t, \tau) = \mathbb{E}\{h^2(t, \tau)\}$. The following corollary provides an analytical expression for $\phi(t, \tau)$.

Corollary 1: $\phi(t, \tau)$ is given by

$$\begin{aligned}
\phi(t, \tau) &= c(t, \tau) \int_0^\infty \left[\exp(-\hat{u}(t, \tau)r_1^2 - \hat{v}(t, \tau)r_1) \right. \\
&\quad \left. - \exp(-\hat{u}(t, \tau)r_1^2 - \hat{w}(t, \tau)r_1) \right] \\
&\quad \times \left(r_1 - 2a_{\text{rx}} + \frac{a_{\text{rx}}^2}{r_1} \right) \mathrm{d}r_1, \quad (14)
\end{aligned}$$

where

$$\begin{aligned}
c(t, \tau) &= \frac{a_{\text{rx}}^2 e^{-\frac{a_{\text{rx}}^2}{2D_1\tau} - \frac{r_0^2}{4D_2t}}}{8D_1\pi\tau^3 r_0 \sqrt{\pi D_2t}}, \quad \hat{u}(t, \tau) = \frac{1}{2D_1\tau} + \frac{1}{4D_2t}, \\
\hat{v}(t, \tau) &= -\frac{a_{\text{rx}}}{D_1\tau} - \frac{r_0}{2D_2t}, \\
\hat{w}(t, \tau) &= -\frac{a_{\text{rx}}}{D_1\tau} + \frac{r_0}{2D_2t}. \quad (15)
\end{aligned}$$

Proof: From the definition, we have

$$\phi(t, \tau) = \mathbb{E}\{h^2(t, \tau)\} = \int_0^\infty h^2(t, \tau) \Big|_{r(t)=r_1} f_{r(t)}(r_1) \mathrm{d}r_1. \quad (16)$$

Substituting (1) and (8) into (16) and simplifying the expression, we obtain (14). ■

Remark 4: The expression in (14) comprises integrals of the form $\int_0^\infty \exp(ax^2 + bx)/x \mathrm{d}x$, where a and b are constants. Such integrals cannot be obtained in closed form. However, the integrals can be evaluated numerically in a straightforward manner.

C. Distribution Functions of the Time-Variant CIR

In this subsection, we derive analytical expressions for the PDF and CDF of $h(t, \tau)$. The PDF of $h(t, \tau)$ is given in the following theorem.

Theorem 2: The PDF of the impulse response of a time-variant channel with diffusive molecules released by a diffusive transparent transmitter and captured by a diffusive absorbing receiver is given by

$$\begin{cases} f_{h(t, \tau)}(h) = \frac{f_{r(t)}(r_1(h))}{\hat{h}'(r_1(h), \tau)} - \frac{f_{r(t)}(r_2(h))}{\hat{h}'(r_2(h), \tau)}, & \text{for } 0 \leq h < h^*, \\ f_{h(t, \tau)}(h) \rightarrow \infty, & \text{for } h = h^*, \\ f_{h(t, \tau)}(h) = 0, & \text{otherwise,} \end{cases} \quad (17)$$

where $\hat{h}(r, \tau)$ denotes $h(t, \tau)$, given by (1), as a function of $r(t)$ and τ , $f_{r(t)}(r)$ is given by (8), $r_1(h)$ and $r_2(h)$, $r_1(h) < r_2(h)$, are the solutions of the equation $\hat{h}(r, \tau) = h$, h^* is the maximum value of $\hat{h}(r, \tau)$ for all values of $r(t)$, and $\hat{h}'(r, \tau)$ is given by

$$\begin{aligned}
\hat{h}'(r, \tau) &= \frac{a_{\text{rx}}}{\sqrt{4\pi D_1\tau^3}} \exp\left(-\frac{(r - a_{\text{rx}})^2}{4D_1\tau}\right) \\
&\quad \times \left(\frac{a_{\text{rx}}}{r^2} - \frac{(r - a_{\text{rx}})}{2D_1\tau} \left(1 - \frac{a_{\text{rx}}}{r}\right) \right). \quad (18)
\end{aligned}$$

Proof: Please refer to Appendix B. ■

As stated in the proof of Theorem 2, there are two different values of $r(t)$, r_1 and r_2 , leading to the same value of $\hat{h}(r, \tau)$, i.e., $h(t, \tau)$, when $0 \leq h < h^*$. Hence, the PDF of $h(t, \tau)$ is a function of the PDFs of these two values of $r(t)$. However, when $h(t, \tau)$ reaches its maximum, $f_{h(t, \tau)}(h)$ approaches infinity and does not depend on $f_{r(t)}(r(h))$ since the probability of $h = h^*$, i.e., $\Pr(h = h^*) = \int_{h^*} f_{h(t, \tau)}(h) \mathrm{d}h$, is finite and $\mathrm{d}h$ approaches 0 at $h = h^*$.

The CDF of $h(t, \tau)$ is given in the following corollary.

Corollary 2: The CDF of the impulse response of a time-variant channel with diffusive molecules released by a diffusive transparent transmitter and captured by a diffusive absorbing receiver is given by

$$\begin{aligned}
F_{h(t, \tau)}(h) &= F_{r(t)}(r_1(h)) + 1 - F_{r(t)}(r_2(h)), \\
&\quad \text{for } 0 \leq h \leq h^*, \quad (19)
\end{aligned}$$

$F_{h(t, \tau)}(h) = 0$, for $h < 0$, and $F_{h(t, \tau)}(h) = 1$, for $h > h^*$, where $F_{r(t)}(r)$ is given by (9).

Proof: From the definition of the CDF and (17), we have

$$\begin{aligned}
F_{h(t, \tau)}(h) &= \int_0^h f_{h(t, \tau)}(\check{h}) \mathrm{d}\check{h} \\
&= \int_0^h \frac{f_{r(t)}(\check{r}_1(\check{h}))}{\partial \hat{h}(\check{r}_1, \tau) / \partial \check{r}_1} - \frac{f_{r(t)}(\check{r}_2(\check{h}))}{\partial \hat{h}(\check{r}_2, \tau) / \partial \check{r}_2} \mathrm{d}\check{h}
\end{aligned}$$

$$\begin{aligned}
&= \int_0^{r_1(h)} f_{r(t)}(\tilde{r}_1) d\tilde{r}_1 - \int_\infty^{r_2(h)} f_{r(t)}(\tilde{r}_2) d\tilde{r}_2 \\
&= F_{r(t)}(r_1(h)) + 1 - F_{r(t)}(r_2(h)), \quad (20)
\end{aligned}$$

where \tilde{r}_1 and \tilde{r}_2 , $\tilde{r}_1 < \tilde{r}_2$, are the solutions of the equation $\tilde{h}(\tilde{r}, \tau) = \tilde{h}$. This completes the proof. ■

Similar to the PDF, the CDF of $h(t, \tau)$ also depends on the CDFs of two values of $r(t)$, i.e., $r_1(h)$ and $r_2(h)$.

D. Distribution Functions of $p(t, T_b)$

Calculating the mean of $p(t, T_b)$ involves an integral of the form $\int_0^\infty \operatorname{erfc}(ax) \exp(-b^2x^2 + cx) dx$, with appropriate constants $a, b, c > 0$, for which a closed-form expression is not known. However, based on the results in Sections III-A and III-C, we obtain the PDF and CDF of $p(t, T_b)$ in the following corollary.

Corollary 3: The PDF and CDF of the probability that a diffusive molecule is absorbed by a diffusive absorbing receiver during an interval T_b after its release at time t by a diffusive transparent transmitter are, respectively, given by

$$f_{p(t, T_b)}(p) = -\frac{f_{r(t)}(\tilde{r}(p))}{p'(\tilde{r})}, \quad (21)$$

$$F_{p(t, T_b)}(p) = 1 - F_{r(t)}(\tilde{r}(p)), \quad (22)$$

where $f_{r(t)}(r)$ and $F_{r(t)}(r)$ are given by (8) and (9), respectively. Here, $\tilde{r}(p)$ is the solution of the equation $p(t, T_b) = p$ and $p'(\tilde{r})$ is given by

$$\begin{aligned}
p'(\tilde{r}) &= -\frac{a_{rx}}{\tilde{r}^2} \operatorname{erfc}\left(\frac{\tilde{r} - a_{rx}}{2\sqrt{D_1 T_b}}\right) \\
&\quad - \frac{a_{rx}}{\tilde{r}\sqrt{\pi D_1 T_b}} \exp\left(-\frac{(\tilde{r} - a_{rx})^2}{4D_1 T_b}\right). \quad (23)
\end{aligned}$$

Proof: The proof of Corollary 3 follows the same steps as the proof of Theorem 2 and Corollary 2 and exploits that $p(t, T_b)$ is a function of $r(t)$ as shown in (4). From (23), we observe that $p'(\tilde{r}) < 0$, so that the equation $p(t, T_b) = p$ has only one solution. Then, we apply the relations for the PDFs and CDFs of functions of random variables [32] to obtain (21) and (22). ■

The mean, variance, PDF, and CDF of $h(t, \tau)$ and $p(t, T_b)$ can be exploited to design efficient and reliable synthetic MC systems. As examples, we consider the design and analysis of drug delivery and MC systems in the following two sections.

IV. DRUG DELIVERY SYSTEM DESIGN

In this section, we apply the derived stochastic parameters of the time-variant CIR for absorbing receivers for the design and performance evaluation of drug delivery systems.

A. Controlled-Release Design

The treatment of many diseases requires the diseased cells to absorb a minimum rate of drugs during a prescribed time period at minimum cost [21]. To design an efficient drug delivery system satisfying this requirement, we minimize the total number of released drug molecules, $A = \sum_{i=1}^I \alpha_i$, subject to the constraint that the absorption rate $g(t)$ is equal to or larger than a target rate, $\theta(t)$, for a period of time, denoted by T_{Rx} .

We allow $\theta(t)$ to be a function of time so that the designed system can satisfy different treatment requirements over time. Since $g(t)$ is random, we cannot always guarantee $g(t) \geq \theta(t)$. Hence, we will design the system based on the first and second order moments of $g(t)$ and use the PDF and CDF of $g(t)$ to evaluate the system performance. In particular, we reformulate the constraint such that the mean of $g(t)$ minus a certain deviation is equal to or above the threshold $\theta(t)$ during T_{Rx} , i.e., $E\{g(t)\} - \beta V\{g(t)\} \geq \theta(t)$, $0 \leq t \leq T_{Rx}$, where $V\{\cdot\}$ denotes standard deviation and β is a coefficient determining how much deviation from the mean is taken into account. Based on (2), the constraint can be written as a function of α_i as follows

$$\begin{aligned}
&E\{g(t)\} - \beta V\{g(t)\} \stackrel{(a)}{\geq} \\
&\sum_{\forall i|t_i < t} \alpha_i (E\{h(t_i, t - t_i)\} - \beta V\{h(t_i, t - t_i)\}) \geq \theta(t), \quad (24)
\end{aligned}$$

for $0 \leq t \leq T_{Rx}$. Inequality (a) in (24) is due to $E\{g(t)\} = E\{\sum_{\forall i|t_i < t} \alpha_i h(t_i, t - t_i)\} = \sum_{\forall i|t_i < t} \alpha_i E\{h(t_i, t - t_i)\}$ and Minkowski's inequality [33]:

$$\begin{aligned}
V\{g(t)\} &= \left[E\left\{ \left(\sum_{\forall i|t_i < t} (\alpha_i h(t_i, t - t_i) \right. \right. \right. \\
&\quad \left. \left. \left. - E\{\alpha_i h(t_i, t - t_i)\} \right)^2 \right\} \right]^{1/2} \\
&\leq \sum_{\forall i|t_i < t} \alpha_i \left[E\left\{ (h(t_i, t - t_i) \right. \right. \right. \\
&\quad \left. \left. \left. - E\{h(t_i, t - t_i)\})^2 \right\} \right]^{1/2} \\
&= \sum_{\forall i|t_i < t} \alpha_i V\{h(t_i, t - t_i)\}. \quad (25)
\end{aligned}$$

Note that we may not be able to find α_i such that (24) holds for all values of β and $\theta(t)$. For example, when β is too large, $E\{g(t)\} - \beta V\{g(t)\}$ can be negative and hence (24) cannot be satisfied for $\theta(t) > 0$. However, when $E\{h(t_i, t - t_i)\} > \beta V\{h(t_i, t - t_i)\}$, i.e., either β or $V\{h(t_i, t - t_i)\}$ are small, such that $\beta V\{h(t_i, t - t_i)\}$ is sufficiently small, we can always find α_i so that (24) holds for arbitrary $\theta(t)$. Since time t is a continuous variable, the constraint in (24) has to be satisfied for all values of t , $0 \leq t \leq T_{Rx}$, and thus there is an infinite number of constraints, each of which corresponds to one value of t . Therefore, we simplify the problem by relaxing the constraints to hold only for a finite number of time instants $t = t_n = n\Delta t_n$, where $n = 1, \dots, N$ and $\Delta t_n = T_{Rx}/N$. Then, the proposed optimization problem for the design of α_i is formulated as follows

$$\begin{aligned}
\min_{\alpha_i \geq 0, \forall i} A &= \sum_{i=1}^I \alpha_i \\
\text{s.t.} \quad &\sum_{i, t_i < t} \alpha_i (m(t_i, n\Delta t_n - t_i) - \beta \sigma(t_i, n\Delta t_n - t_i)) \\
&\geq \theta(n\Delta t_n), \text{ for } n = 1, \dots, N, \quad (26)
\end{aligned}$$

where $m(t, \tau)$ and $\sigma(t, \tau)$ are the mean (11) and the standard deviation (13) of $h(t, \tau)$, respectively. Since $m(t, \tau)$ and $\sigma(t, \tau)$ do not oscillate but are well-behaved and smooth functions of t as shown in Section VI, a small value of N (e.g., $N = 5$) is usually enough to meet the continuous constraint (24) for all t . Having $m(t, \tau)$ in (11) and $\sigma(t, \tau)$ in (13) and treating the α_i as real numbers, (26) can be readily solved numerically as a linear program. We note that although the numbers of drug molecules α_i are integers, for tractability, we solve (26) for real α_i and quantize the results to the nearest integer values.

We note that the problem in (26) is statistical in nature and provides guidance for the offline design of the drug delivery system.²

B. System Performance

Since $g(t) \geq \theta(t)$ is required for proper operation of the system, we evaluate the system performance in terms of the probability that the drug absorption rate satisfies the target rate $g(t) \geq \theta(t)$, denoted by $P_\theta(t) = \Pr\{g(t) \geq \theta(t)\}$. $P_\theta(t)$ is given in the following theorem.

Theorem 3: The system performance metric $P_\theta(t)$ can be expressed as

$$P_\theta(t) = 1 - f_{\alpha_1 h(t_1, t-t_1)}(\theta(t)) * \dots * f_{\alpha_{i-1} h(t_{i-1}, t-t_{i-1})}(\theta(t)) * F_{\alpha_i h(t_i, t-t_i)}(\theta(t)), \quad (27)$$

where $*$ denotes convolution, and $i = 1, 2, \dots$ satisfies $t_i \leq t$. In (27), we define $f_{\alpha_i h(t_i, t-t_i)}(\theta(t)) = 1/\alpha_i \times f_{h(t_i, t-t_i)}(\theta(t)/\alpha_i)$ and $F_{\alpha_i h(t_i, t-t_i)}(\theta(t)) = F_{h(t_i, t-t_i)}(\theta(t)/\alpha_i)$.

Proof: From the definition of the CDF, we have

$$P_\theta(t) = 1 - F_{g(t)}\{\theta(t)\} = 1 - \int_0^{\theta(t)} f_{g(t)}(g) \, dg. \quad (28)$$

Due to the summation of independent random variables in (2), i.e., independent releases at t_i , we have

$$f_{g(t)}(g) = \left(f_{\alpha_1 h(t_1, t-t_1)} * \dots * f_{\alpha_i h(t_i, t-t_i)} \right)(g). \quad (29)$$

Substituting (29) into (28), then using the integration property of the convolution, i.e.,

$$\begin{aligned} & \int_0^{\theta(t)} \left(f_{\alpha_1 h(t_1, t-t_1)} * \dots * f_{\alpha_i h(t_i, t-t_i)} \right)(g) \, dg \\ &= f_{\alpha_1 h(t_1, t-t_1)}(\theta(t)) * \dots * \int_0^{\theta(t)} f_{\alpha_i h(t_i, t-t_i)}(g) \, dg, \end{aligned} \quad (30)$$

and using the definition of the CDF, we obtain (27). ■

We note that the analytical expressions for the PDF and CDF of $h(t, \tau)$ in Theorem 2 and Corollary 2, respectively, are not in closed form. Nevertheless, the evaluation of the system performance in (27) can be approximated by a discrete convolution which can be easily evaluated numerically.

²In practice, when designing a system in a dynamic environment, one would adopt typical values of environment parameters for the offline design.

Furthermore, we note that a minimum value of $P_\theta(t)$ can be guaranteed based on the statistical moments of the CIR without knowledge of the PDF and the CDF as shown in the following proposition.

Proposition 1: For a given solution of (24), a lower bound on $P_\theta(t) = \Pr\{g(t) \geq \theta(t)\}$ is given as follows

$$P_\theta(t) \geq 1 - \frac{1}{\beta^2}. \quad (31)$$

Proof: By using (24) and the Chebyshev inequality [34], we obtain

$$\begin{aligned} P_\theta(t) & \stackrel{(a)}{\geq} \Pr\{|g(t) - E\{g(t)\}| \leq E\{g(t)\} - \theta(t)\} \\ & \stackrel{(b)}{\geq} 1 - \frac{V^2\{g(t)\}}{(E\{g(t)\} - \theta(t))^2} \stackrel{(c)}{\geq} 1 - \frac{1}{\beta^2}, \end{aligned} \quad (32)$$

where (a) can be obtained by expanding the absolute value on the right-hand side, (b) is due to the Chebyshev inequality, and (c) is due to (24). This completes the proof. ■

Remark 5: Proposition 1 is not only useful for evaluating the system performance, but also provides a guideline for the design of the release profile of drugs in (26). For example, to ensure a high absorption rate probability of $P_\theta(t) \geq 0.75$, from (31), we need to set the β coefficient in (26) as $\beta = 2$. Note that a useful bound can only be obtained based on (31) when $\beta > 1$ and (24) is satisfied.

V. MC SYSTEM DESIGN FOR IMPERFECT CSI

In this section, we apply the stochastic analysis presented in Section III for the design of MC systems with imperfect CSI. The CSI is imperfect due to the movement of the transceivers and assumed to be known only at the beginning of a bit frame. In particular, we optimize three design parameters of a diffusive mobile MC system employing on-off keying modulation and threshold detection, namely the detection threshold at Rx, the release profile at Tx, and the time duration of a bit frame. By choosing the optimal values of those three parameters, we can improve the system performance while keeping the overall system relatively simple. First, we optimize the detection threshold for minimization of the maximum BER in a frame assuming a uniform release profile. This approach can be employed in very simple MC systems where Tx is not capable of adjusting the number of released molecules. Second, we optimize the release profile at Tx for minimization of the maximum BER in a frame, assuming a fixed detection threshold and a fixed number of molecules available for transmission in the frame. This second approach to MC optimization improves the system performance in terms of BER but requires a mechanism to control the number of molecules released at Tx. Third, we design the optimal duration of the bit frame satisfying a constraint on the efficiency of molecule usage. Thus, this third approach improves the system performance in terms of the efficiency of molecule usage. The three proposed designs can be performed offline. Furthermore, they can be combined with each other or carried out separately depending on the capabilities and requirements of the system. For all three designs, as a first step, we need to derive the BER as a function of the number of released molecules.

A. Detection and BER

We consider a simple threshold detector at Rx, where the received signal q_i is compared with a detection threshold, denoted by ξ , in order to determine the detected bit \hat{b}_i as follows

$$\hat{b}_i = \begin{cases} 1 & \text{if } q_i > \xi, \\ 0 & \text{if } q_i \leq \xi. \end{cases} \quad (33)$$

Given the assumption of no ISI and $\Pr(\tilde{b}_i) = 1/2$, from (3) and (33), the error probability of the i -th bit, denoted by $P_b(b_i)$, can be simplified as [27, eq. (12)]

$$P_b(b_i) = \frac{1}{2} - \frac{1}{4} \operatorname{erf}\left(\frac{\xi - \eta}{\sqrt{2\eta}}\right) + \frac{1}{4} \int_0^\infty f_{r(t)}(r_i) \operatorname{erf}(\zeta_i(\xi, \alpha_i)) d r_i, \quad (34)$$

where $f_{r(t)}(r_i)$ is given in (8), r_i is $r(t_i)$ for brevity, and $\zeta_i(\xi, \alpha_i) = \frac{\xi - \mu_{i,1}}{\sigma_{i,1}\sqrt{2}} = \frac{\xi - (\alpha_i p(t_i, T_b) + \eta)}{\sqrt{2(\alpha_i p(t_i, T_b)(1 - p(t_i, T_b)) + \eta)}}$. Note that $P_b(b_i)$ depends on i since the distance $r(t_i)$ between the transceivers is a function of release time t_i .

B. Optimal Detection Threshold for Uniform Release

We first consider system design for uniform release, where the number of available molecules is uniformly allocated across all bits of a frame. To facilitate reliable communication, our objective is to optimize the detection threshold, ξ , such that the maximum value of the error rate of the bits in a frame is minimized, given the total number of available molecules in a frame, A , i.e.,

$$\min_{\xi} \max_i \{P_b(b_i)\} \text{ s.t. } \alpha_i = A/I. \quad (35)$$

From (34), the problem is equivalent to

$$\min_{\xi} \max_i \left\{ \int_0^\infty f_{r(t)}(r_i) \operatorname{erf}(\zeta_i(\xi, \alpha_i)) d r_i - \operatorname{erf}\left(\frac{\xi - \eta}{\sqrt{2\eta}}\right) \right\} \text{ s.t. } \alpha_i = A/I. \quad (36)$$

The following lemma reveals the convexity of the problem in (36).

Lemma 2: For $\eta < \xi < \mu_{i,1}$, the objective function in (36) is convex in ξ .

Proof: Please refer to Appendix C. ■

Note that $\eta < \xi < \mu_{i,1}$ is intuitively satisfied for typical system parameters since the decision threshold should be higher than the average noise level when bit “0” is sent but should not exceed the mean of the received signal when bit “1” is sent. Otherwise, a high error rate would result. Due to the convexity of problem (36), the global optimum ξ can be easily obtained by numerical methods such as the interior-point method [32].

C. Optimal Release With Fixed Detection Threshold

For the second proposed design, we aim to optimize the release profile, i.e., the number of molecules available for release for each bit, α_i , such that $\max_i \{P_b(b_i)\}$ is minimized

given a total number of molecules A that are available for release in a frame

$$\min_{\alpha} \max_i \{P_b(b_i)\} \text{ s.t. } \sum_{i=1}^I \alpha_i = A, \quad (37)$$

where $\alpha = [\alpha_1, \alpha_2, \dots, \alpha_I]$.

For a given threshold ξ , we can re-express (37) based on (34) as follows

$$\min_{\alpha} \max_i \left\{ \int_0^\infty f_{r(t)}(r_i) \operatorname{erf}(\zeta_i(\xi, \alpha_i)) d r_i \right\} \text{ s.t. } \sum_{i=1}^I \alpha_i = A. \quad (38)$$

The following lemma states the convexity of the optimization problem in (38).

Lemma 3: For $\eta < \xi < \mu_{i,1}$, the objective function in (38) is convex in α .

Proof: Please refer to Appendix D. ■

Hence, the global optimum of (38) can be readily obtained by numerical methods such as the interior-point method.

Note that, for tractability, similar to the proposed drug delivery design, we solve (36) and (38) for real α_i and quantize the results to the nearest integer values.

D. Optimal Time Duration of a Bit Frame

In the third proposed design, we consider the molecule usage efficiency for communication. We evaluate the efficiency based on $p(t, T_b)$, i.e., the probability that a signaling molecule is absorbed during bit interval T_b after its release at time t . If $p(t, T_b)$ is too small, none of the released molecules may actually reach the receiver and thus the molecules are wasted, i.e., the system has low efficiency. Hence, we want to keep $p(t, T_b)$ above a certain value, denoted by ψ . Intuitively, as on average $h(t, \tau)$ decreases over time t , $p(t, T_b)$, which is the integral over $h(t, \tau)$ with respect to τ , also on average decreases over time. Therefore, our objective is to choose the maximum duration of a bit frame, denoted by T^* , such that $p(t, T_b) > \psi$ for $t \leq T^* - T_b$, where t is the release time.

Since $p(t, T_b)$ is a random process, we cannot enforce $p(t, T_b) > \psi$ but can only bound the probability that $p(t, T_b) > \psi$ is satisfied, i.e., $\Pr(p(t, T_b) > \psi) \geq P$, where P is a design parameter. Moreover, we have

$$\Pr(p(t, T_b) > \psi) = 1 - F_{p(t, T_b)}(\psi) \stackrel{(a)}{=} F_{r(t)}(\tilde{r}(\psi)), \quad (39)$$

where equality (a) is due to (22). As such, we can re-express the problem as maximizing the duration of a bit frame such that $F_{r(t)}(\tilde{r}(\psi)) \geq P$ holds. To this end, in the following lemma, we analyze $F_{r(t)}(\tilde{r}(\psi))$ as a function of time t .

Lemma 4: $F_{r(t)}(\tilde{r}(\psi))$ is a decreasing function of time t .

Proof: Please refer to Appendix E. ■

Since Lemma 4 shows that $F_{r(t)}(\tilde{r}(\psi))$ is a decreasing function of time, the maximum duration of a bit frame satisfying $F_{r(t)}(\tilde{r}(\psi)) \geq P$ can be found by solving $F_{r(T^* - T_b)}(\tilde{r}(\psi)) = P$, where $F_{r(T^* - T_b)}(\tilde{r}(\psi))$ is given in (9).

TABLE I
SYSTEM PARAMETERS USED FOR NUMERICAL RESULTS

Parameter	Value	Parameter	Value
D_{Tx} [m ² /s]	1×10^{-14}	D_{Rx} [m ² /s]	0
D_x [m ² /s]	8×10^{-11}	r_0 [m]	10×10^{-6}
a_{tx} [m]	1×10^{-7}	a_{rx} [m]	1×10^{-6}
T [h]	24	T_{Rx} [h]	24
I	3000	N	5
T_b [s]	28.8	$\theta(t)$ [s ⁻¹]	1

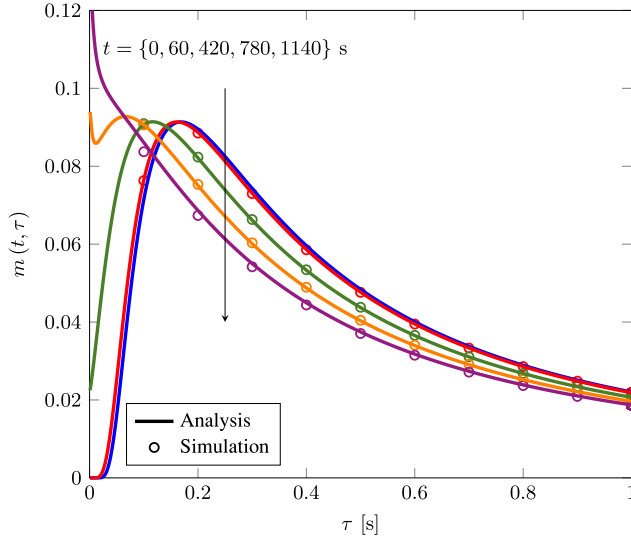


Fig. 2. Mean of the CIR $h(r(t), \tau)$ as a function of time τ .

Remark 6: If multiple frames are transmitted, the proposed design framework can be applied to each frame, respectively. However, the optimal designs may be different for different frames due to the moving transceivers, whose distances are assumed to be perfectly estimated at the start of each frame.

Remark 7: Here, we discuss a system with an absorbing receiver. Nevertheless, the proposed optimal design framework can also be applied to transparent receivers. For a transparent receiver, $p(t, T_b)$ is the probability that a molecule is observed inside the volume of the transparent receiver at time T_b after its release at time t at the center of Tx.

VI. NUMERICAL RESULTS

In this section, we provide numerical results to evaluate the accuracy of the derived expressions and analyze the performance of the MC systems in the considered application scenarios. We use the set of simulation parameters summarized in Table I, unless stated otherwise. The parameters are chosen to match the actual system parameters in drug delivery systems, as will be explained in detail in Section VI-B.

A. Time-Variant Channel Analysis

In this subsection, we numerically analyze the time-variant MC channel. For verification of the accuracy of the expressions derived in Section III, we employ a hybrid particle-based simulation approach. In particular, we use particle-based simulation of the Brownian motion of the transceivers to generate

realizations of the random distance between Tx and Rx, $r(t)$. Then, we use Monte Carlo simulation to obtain the desired statistical results by suitably averaging the CIRs (1) obtained for the realizations of $r(t)$. For particle-based simulation of the Brownian motion of Tx, Tx performs a random walk with a random step size in space in every discrete time step of length $\Delta t^{\text{st}} = 1$ ms. The length of each step in space is modeled as a Gaussian random variable with zero mean and standard deviation $\sqrt{2D_{Tx}\Delta t^{\text{st}}}$. Furthermore, we also take into account the reflection of Tx upon collision with Rx. When Tx hits Rx, we assume that it bounces back to the position it had at the beginning of the considered simulation step [30].

Fig. 2 shows the mean of the CIR, $m(t, \tau)$, as a function of τ . In general, for large τ , $m(t, \tau)$ decreases when t increases as expected since the transceivers move away from each other on average. For large τ , $m(t, \tau)$ also decreases when τ increases as would be the case in a static system. In drug delivery systems, the decrease of $m(t, \tau)$ means that the average amount of drugs delivered to the tumor cells is reduced. In MC, the decrease of $m(t, \tau)$ corresponds to fewer received signaling molecules, and thus a higher BER. Note that in the simulations, unlike the analysis, we have taken into account the reflection of Tx when it hits Rx. Therefore, the good agreement between simulation and analytical results in Fig. 2 suggests that the reflection of Tx does not have a significant impact on the statistical properties of $h(t, \tau)$ and the approximation in (8) and the analytical results obtained based on it are valid.

In Fig. 3, we plot the PDF of the CIR for time instances $t = \{36, 360, 3600\}$ s and $\tau = 0.17$ s. Fig. 3 shows that when t increases, a smaller value of $h(t, \tau)$ is more likely to occur since, on average, the transceivers move away from each other. When t is very large, it is likely that the molecules cannot reach Rx, and hence, cannot be absorbed, consequently $h(t, \tau) \rightarrow 0$. We also observe that $h(t, \tau)$ has a maximum value and $f_{h(t, \tau)}(h(t, \tau)) \rightarrow \infty$ when $h(t, \tau)$ approaches the maximum value as stated in (17). For example, $h(t = 36$ s, $\tau = 0.17$ s) is random but its maximum possible value is 0.29 and $f_{h(t=36 \text{ s}, \tau=0.17 \text{ s})}(0.29) \rightarrow \infty$.

Figs. 2 and 3 show a perfect match between simulation and analytical results. This confirms the accuracy of our analysis of the time-variant CIR in Section III. Note that although the derived analytical expressions for the statistical parameters of the channel are quite involved, insight regarding the impact of the system parameters on the behavior of the channel can be obtained by plotting the analytical expressions, see Figs. 2 and 3. The same results can also be obtained via particle-based simulation. However, this is very time consuming and evaluating the derived analytical expressions is orders of magnitude faster. Since particle-based simulation is costly, in the following subsections, we adopt Monte-Carlo simulation by averaging our results, i.e., $g(t)$ in Figs. 5 and 6, BER in Fig. 8, and $p(t, T_b)$ in Fig. 9, over 10^5 independent realizations of both the distance $r(t)$ and the CIR. The distance $r(t)$ is calculated from the locations of the transceivers, which are generated from Gaussian distributions, see Section III-A. In particular, $r(t) = \sqrt{\sum_{d \in \{x, y, z\}} (r_{d, Rx}(t) - r_{d, Tx}(t))^2}$, where $r_{d, Tx}(t) \sim \mathcal{N}(r_{d, Tx}(t = 0), 2D_{Tx}t)$, $r_{d, Rx}(t) \sim$

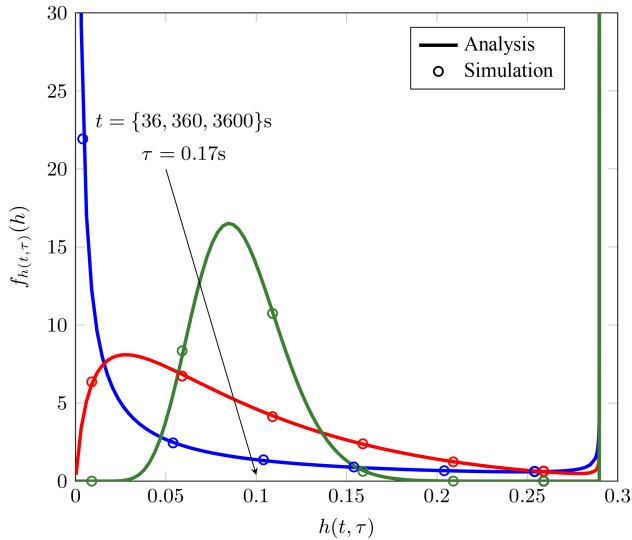


Fig. 3. PDF of the CIR $f_{h(t,\tau)}(h)$ for $\tau = 0.17$ s and $t = \{36,360,3600\}$ s.

$\mathcal{N}(r_{d,Rx}(t=0), 2D_{Rx}t)$, $r_{d,Tx}(t=0) = 0$, and $r_{d,Rx}(t=0) = 1/\sqrt{3}r_0$. The CIR is given by (1) for each realization of $r(t)$.

B. Drug Delivery System Design

In this section, we provide numerical results for the considered drug delivery system. As mentioned above, the parameters in Table I are chosen to match real system parameters, e.g., the diffusion coefficient D_X of drug molecules vary from 10^{-9} to 10^{-14} m²/s [20], drug carriers have sizes $a_{tx} \geq 100$ nm [18], the size of tumor cells is on the order of μm , and drug carriers can be injected or extravasated from the cardiovascular system into the tissue surrounding the targeted diseased cell site [19], i.e., close to the tumor cells. The dosing periods in drug delivery systems are on the order of days [35], i.e., 24 h. Given $T = 24$ h, we choose I relatively large to obtain small intervals T_b . For simplicity, we set $N = 5$, as suggested in Section IV-A, and the value of the required absorption rate is set to $\theta(t) = 1 \text{ s}^{-1}$.

In Fig. 4, we plot the number of released molecules α_i versus the corresponding release time t_i [h] for different system parameters. The coefficients are obtained by solving the optimization problem in (26) with $\beta = \{0,0.4,1,2\}$ for $D_{Tx} = 10^{-14}$ m²/s and $\beta = \{0,0.4\}$ for $D_{Tx} = \{5,10\} \times 10^{-14}$ m²/s. As mentioned in the discussion of (24), we cannot choose large values of β when the diffusion coefficient is large, i.e., the standard deviation is large, as the problem in (26) may become infeasible. Fig. 4 shows that for all considered parameter settings, we first have to release a large number of molecules for the absorption rate to exceed the threshold. Then, in the static system with $D_{Tx} = 0$ m²/s, the optimal coefficient decreases with increasing time, since a fraction of the molecules previously released from Tx linger around Rx and are absorbed later. However, for the time-variant channel, Tx eventually diffuses away from Rx as time t increases and hence, molecules released at later times by Tx will be far away from Rx and may not reach it. Therefore, at

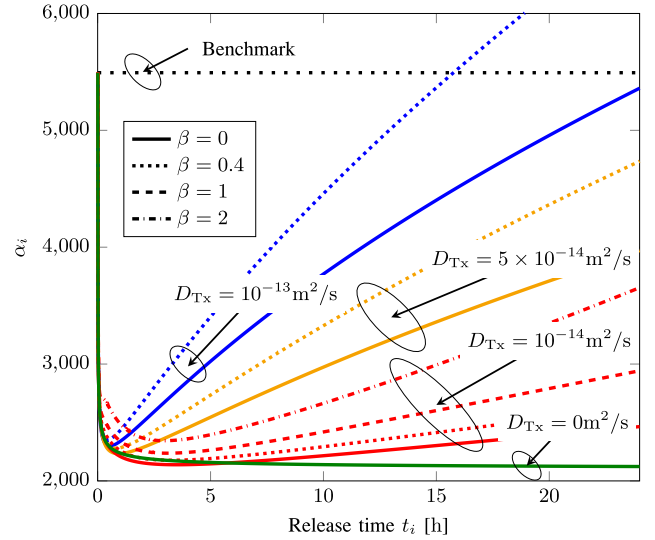


Fig. 4. Optimal number of released molecules α_i as a function of release time t_i [h] for different system parameters and $T = 24$ h. The black horizontal dotted line is the benchmark when the α_i are not optimized.

later times, the amount of drugs released has to be increased for the absorption rate to not fall below the threshold. For larger D_{Tx} , Tx diffuses away from Rx faster and thus, the number of released molecules α_i have to increase faster. This type of drug release, i.e., first releasing a large amount of drugs, then reducing and eventually increasing the amount of released drugs again, is called a tri-phasic release [36]. Once we have designed the release profile, we can implement it by choosing a suitable drug carrier as shown in [36]. Moreover, as expected, for larger β , we need to release more drugs to ensure that (26) is feasible. The black horizontal dotted line in Fig. 4 is a benchmark where the $\alpha_i, \forall i$, are not optimized but naively set to $\alpha_i = \alpha_1 = 5493$. For this naive design, $A = \alpha_1 I \approx 1.65 \times 10^7$, whereas with the optimal α_i , for $\beta = 0$ and $D_{Tx} = 10^{-13}$ m²/s, $A = 1.2 \times 10^7$, i.e., 27% less than the A required for the naive design, and for $\beta = 1$ and $D_{Tx} = 10^{-14}$ m²/s, $A = 7.6 \times 10^6$, i.e., 54% less than the A required for the naive design. This highlights that applying the optimal release profile can save significant amounts of drugs and still satisfy the therapeutic requirements. Moreover, as observed in Fig. 4, at later times, e.g., $t_i > 15$ h for $D_{Tx} = 10^{-13}$ m²/s, the values of α_i required to satisfy the desired absorption rate are higher than the fixed α_i used in the naive design, i.e., the benchmark, which means that the naive design cannot provide the required absorption rate.

In Fig. 5, we plot the mean and standard deviation of the absorption rate, $E\{g(t)\}$ and $V\{g(t)\}$, between the 1000-th release and the 1002-th release for three designs. For designs 1 and 2, we assumed $D_{Tx} = 10^{-13}$ m²/s and $\beta = 0$, and for design 3, we adopted $D_{Tx} = 10^{-14}$ m²/s and $\beta = 1$. Note that the considered time window, e.g., between the 1000-th release and the 1002-th release, is chosen arbitrarily in the middle of T to analyze the system behavior between individual releases. For design 1, Tx diffuses with $D_{Tx} = 10^{-13}$ m²/s but the release profile is designed without accounting for Tx's mobility, i.e., the adopted α_i are given by the green line in Fig. 4 obtained under the assumption of $D_{Tx} = 0$ m²/s.

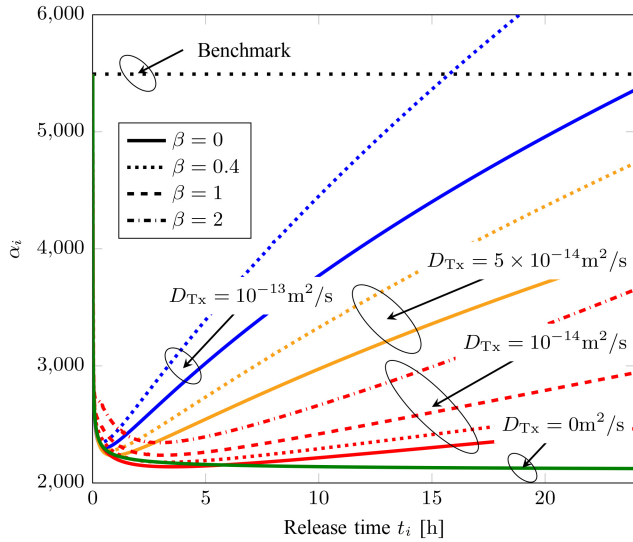


Fig. 5. $E\{g(t)$ and $V\{g(t)$ between the 1000-th release and the 1002-th release, i.e., at about 8 h, for three different designs. Design 1 (green line): naive design without considering Tx's movement with $D_{Tx} = 10^{-13} \text{ m}^2/\text{s}$ and $\beta = 0$; design 2 (blue line) and 3 (red line): optimal design for $(D_{Tx}[\text{m}^2/\text{s}], \beta) = (10^{-13}, 0)$, and $(10^{-14}, 1)$, respectively.

For designs 2 and 3, the mobility of Tx is taken into account. The black dashed line marks the threshold $\theta(t)$ that $g(t)$ should not fall below. It is observed from Fig. 5 that when Tx diffuses but the design does not take into account the mobility, the requirement that the expected absorption rate, $E\{g(t)$, exceeds $\theta(t)$, is not satisfied for most of the time, i.e., the treatment might be unsuccessful. For design 2 with $\beta = 0$, we observe that $E\{g(t) > \theta(t)$ always holds but $E\{g(t) - V\{g(t) > \theta(t)$ does not always hold, which means that while the received amount of drugs on average exceeds the treatment requirement, it varies, and thus, at some times, it may not satisfy the treatment requirement. For design 3 with $\beta = 1$, we observe that $E\{g(t) - V\{g(t) > \theta(t)$ always holds since $\beta > 0$ enforces a gap between $E\{g(t)$ and $\theta(t)$. In other words, even if $g(t)$ deviates from the mean, it can still exceed $\theta(t)$, i.e., even if the received amount of drugs varies, the treatment requirement is still likely satisfied.

In Fig. 6, we present the system performance in terms of the probability that $g(t) \geq \theta(t)$, $P_\theta(t)$, for the time period between the 1000-th and 1002-th releases, i.e., at about 8 h. The lines and markers denote simulation and analytical results for different values of β and D_{Tx} , respectively. To avoid overloading the figure, we show analytical results, given by (27), only for the cases $\beta = 0$, $D_{Tx} = 1 \times 10^{-13} \text{ m}^2/\text{s}$, and $D_{Tx} = 5 \times 10^{-14} \text{ m}^2/\text{s}$. For these cases, Fig. 6 shows a good agreement between analytical and simulation results. In Fig. 6, we observe that $P_\theta(t)$ increases with increasing β because the design for larger β enforces a larger gap between $E\{g(t)$ and $\theta(t)$, as can be seen in Fig. 5. Moreover, for a given β , $P_\theta(t)$ will be different for different D_{Tx} . In particular, for larger D_{Tx} , $P_\theta(t)$ is smaller due to the faster diffusion and increasing randomness of the CIR. Moreover, in Fig. 6, the green line shows that the naive design, i.e., design 1 in Fig. 5, has very poor performance. In Fig. 6, we also observe that between two releases, $P_\theta(t)$ first increases due to the released

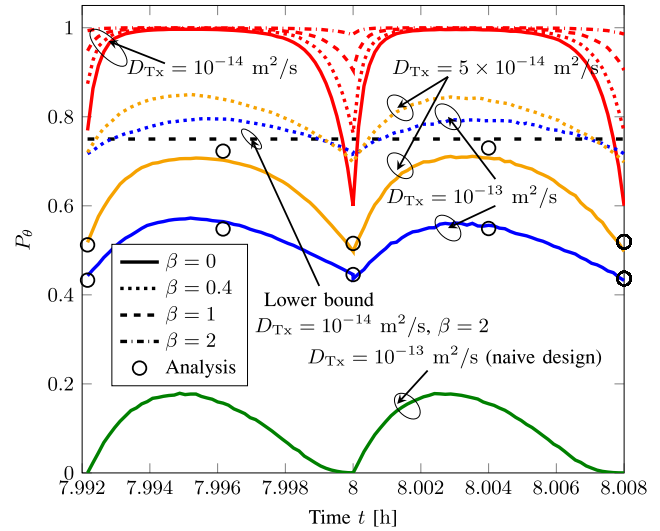


Fig. 6. $P_\theta(t)$ as a function of time t [h] between the 1000-th release and the 1002-th release, i.e., at about 8 h.

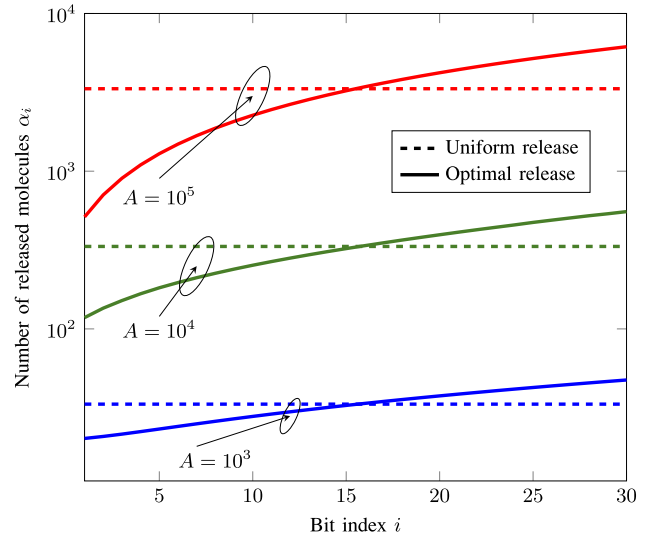


Fig. 7. The number of molecules available for release for each bit for uniform and optimal release when $A = \{10^3, 10^4, 10^5\}$ and $T = 300$ s.

drugs and then decreases due to drug diffusion. Furthermore, in Fig. 6, we also show the lower bound on $P_\theta(t)$ derived in Proposition 1 for $D_{Tx} = 10^{-14} \text{ m}^2/\text{s}$ and $\beta = 2$, where (31) yields $P_\theta(t) \geq 0.75$. Fig. 6 shows that the red dash-dotted line, i.e., $P_\theta(t)$ for $D_{Tx} = 10^{-14} \text{ m}^2/\text{s}$ and $\beta = 2$, is indeed above the horizontal black dashed line, i.e., $P_\theta(t) = 0.75$.

C. Molecular Communication System Design

In this subsection, we show numerical results for the second application scenario, i.e., an MC system with imperfect CSI. We apply again the system parameters in Table I except that here we set $D_{Rx} = 10^{-11} \text{ m}^2/\text{s}$, $I = 30$, $\eta = 1$, $T = 300$ s, and $T_b = T/I = 10$ s to also allow Rx to move and to reduce the transmission window compared to the drug delivery system.

In Fig. 7, we consider the optimal release design, i.e., the optimal number of molecules available for transmission of each bit in a frame, for an MC system with fixed detection

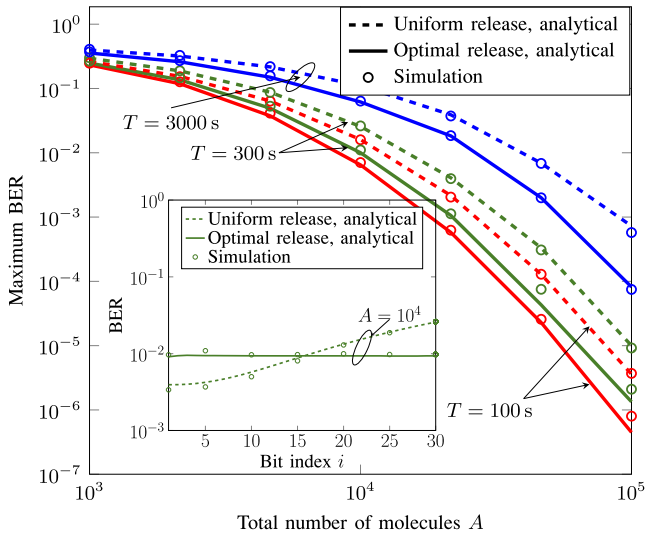


Fig. 8. Maximum BER in a frame as a function of A with uniform and optimal release. The inset shows the BER for each bit in a frame for uniform and optimal release for $A = 10^4$ and $T = 300$ s.

thresholds and fixed A , $A = \{10^3, 10^4, 10^5\}$. The fixed detection thresholds ξ are obtained from Section V-B by assuming uniform release. Fig. 7 reveals that in order to minimize the maximum BER in a frame, the optimal release profile increases over the frame duration, i.e., the number of released molecules is smaller at the beginning of the frame and gradually increases over time. This is expected since, on average, for later release times, more molecules are needed to compensate for the increasing distance between the transceivers.

Fig. 8 shows the maximum BER within a frame for uniform release and the proposed release design obtained from (38), with a fixed detection threshold obtained from (36), as a function of A for $T = \{100, 300, 3000\}$ s. As can be observed, the proposed optimal release profile leads to significant performance improvements compared to uniform release, especially for large A . For example, for $A = 10^5$ and $T = 3000$ s, the maximum BER is reduced by a factor of 8 for optimal release compared to uniform release. On the other hand, to achieve a given desired BER, the total number of molecules A required for optimal release is lower than that for uniform release. In the inset of Fig. 8, we show the BER as a function of bit index i in one frame for uniform and optimal release for $A = 10^4$ and $T = 300$ s. We observe that the optimal release achieves a lower maximum BER compared to the uniform release. We also observe that the optimal release leads to approximately the same BER for each bit in a frame which highlights the benefits of the proposed design. Note that if the transceivers are diffusive but the stochasticity of the channel is not taken into account, one may adopt a uniform release, which is optimal for static transceivers. However, this would lead to a considerable performance reduction compared to the optimized release. Furthermore, for uniform release, for the static channel model, one would expect the BER to be identical for all bits. This leads to incorrect results. For example, in the inset of Fig. 8, for uniform release the BER of the 30-th bit would be predicted equal to the BER of the 1-st bit, i.e., 4×10^{-3} , instead of the real value of 2.6×10^{-1} .

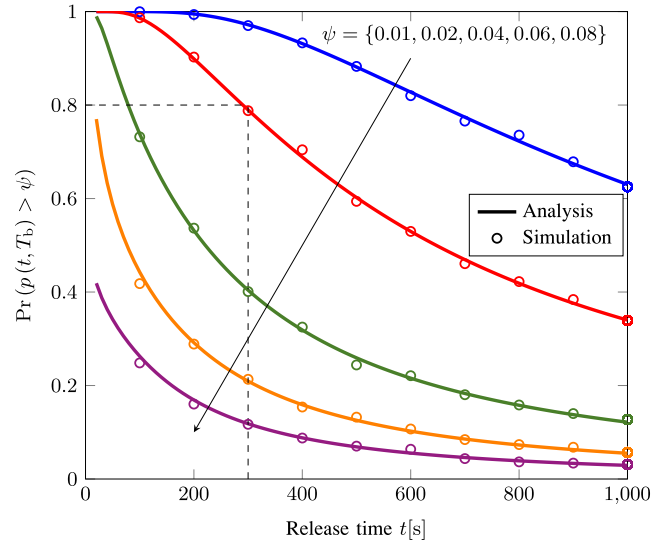


Fig. 9. The probability that $p(t, T_b)$ is larger than a given value ψ as a function of t for $T_b = 10$ s.

Fig. 9 shows the probability that $p(t, T_b)$ is larger than a given value ψ , $\Pr(p(t, T_b) > \psi)$, as a function of time t . $\Pr(p(t, T_b) > \psi)$ provides information about the probability that a released molecule is absorbed at the Rx, i.e., the efficiency of molecule usage. We observe from Fig. 9 that $\Pr(p(t, T_b) > \psi)$ is a decreasing function of time as expected from the analysis in Section V-D. Moreover, for a given t , $\Pr(p(t, T_b) > \psi)$ is smaller for larger ψ . Furthermore, we can deduce the maximum time duration of a bit frame, T^* , satisfying a required molecule usage efficiency from Fig. 9. For example, for $t \leq 300$ s, $\Pr(p(t, T_b) > 0.02) \geq 0.8$ holds. Thus, $T^* = t + T_b = 310$ s guarantees a molecule usage efficiency of $\Pr(p(t, T_b) > 0.02) \geq 0.8$.

VII. CONCLUSION

In this paper, we considered a diffusive mobile MC system with an absorbing receiver, in which both the transceivers and the molecules diffuse. We provided a statistical analysis of the time-variant CIR and its integral, i.e., the probability that a molecule is absorbed by Rx during a given time period. We applied this statistical analysis to two system design problems, namely drug delivery and on-off keying based MC with imperfect CSI. For the drug delivery system, we proposed an optimal release profile which minimizes the number of released drug molecules while ensuring a target absorption rate for the drugs at the diseased site during a prescribed time period. The probability of satisfying the constraint on the absorption rate was adopted as a system performance criterion and evaluated. We observed that ignoring the reality of the Tx's mobility for designing the release profile leads to unsatisfactory performance. For the MC system with imperfect CSI, we optimized three design parameters, i.e., the detection threshold at Rx, the release profile at Tx, and the time duration of a bit frame. Our simulation results revealed that the proposed MC system designs achieved a better performance in terms of BER and molecule usage efficiency compared to a uniform-release system and a system without limitation on

molecule usage, respectively. Overall, our results showed that taking into account the time-variance of the channel of mobile MC systems is crucial for achieving high performance.

APPENDIX A
PROOF OF LEMMA 1

To prove (6), we have

$$\begin{aligned}
\mathbb{E}\{r(t)\} &\stackrel{(a)}{=} \sqrt{2D_2t} \mathbb{E}\{\gamma\} \\
&\stackrel{(b)}{=} \sqrt{2D_2t} \sqrt{2} e^{-\frac{\lambda^2}{2}} \sum_{n=0}^{\infty} \frac{\Gamma(n+2)}{n! \Gamma(n+3/2)} \left(\frac{\lambda^2}{2}\right)^n \\
&= \sqrt{\frac{D_2t}{\pi}} 4e^{-\frac{\lambda^2}{2}} \sum_{n=0}^{\infty} \frac{(n+1)!}{(2n+1)!} (2\lambda^2)^n \\
&= \sqrt{\frac{D_2t}{\pi}} 2e^{-\frac{\lambda^2}{2}} \sum_{n=0}^{\infty} \left(\frac{(n)!}{(2n)!} + \frac{(n)!}{(2n+1)!} \right) (2\lambda^2)^n \\
&\stackrel{(c)}{=} \sqrt{\frac{D_2t}{\pi}} 2e^{-\frac{\lambda^2}{2}} \left(1 + \frac{\sqrt{\pi}}{2} \sqrt{2\lambda^2} e^{\frac{\lambda^2}{2}} \operatorname{erf}\left(\frac{\lambda}{\sqrt{2}}\right) \right. \\
&\quad \left. + \frac{\sqrt{\pi}}{\sqrt{2\lambda^2}} e^{\frac{\lambda^2}{2}} \operatorname{erf}\left(\frac{\lambda}{\sqrt{2}}\right) \right), \quad (40)
\end{aligned}$$

where $\Gamma(\cdot)$ denotes the Gamma function, equality (a) is due to (5), equality (b) is due to [37, Eq. (1.5)], and equality (c) is obtained by applying [31, eq. (5.2.11.6) and eq. (5.2.11.7)]. Simplifying the final expression, we obtain (6).

To prove (7), we have

$$\begin{aligned}
\mathbb{E}\{r^2(t)\} &\stackrel{(a)}{=} 2D_2t \mathbb{E}\{\gamma^2\} \\
&\stackrel{(b)}{=} 2D_2t 2e^{-\frac{\lambda^2}{2}} \sum_{n=0}^{\infty} \frac{\Gamma(n+5/2)}{n! \Gamma(n+3/2)} \left(\frac{\lambda^2}{2}\right)^n \\
&= 4D_2t e^{-\frac{\lambda^2}{2}} \left(\frac{\lambda^2}{2} \sum_{n=1}^{\infty} \frac{1}{(n-1)!} \left(\frac{\lambda^2}{2}\right)^{n-1} \right. \\
&\quad \left. + \frac{3}{2} \sum_{n=0}^{\infty} \frac{1}{n!} \left(\frac{\lambda^2}{2}\right)^n \right) \\
&\stackrel{(c)}{=} 4D_2t e^{-\frac{\lambda^2}{2}} \left(\frac{\lambda^2}{2} e^{\frac{\lambda^2}{2}} + \frac{3}{2} e^{\frac{\lambda^2}{2}} \right) = r_0^2 + 6D_2t, \quad (41)
\end{aligned}$$

where equality (a) is obtained due to (5), equality (b) is due to [37, eq. (1.5)], and equality (c) is obtained by applying the Maclaurin series of the exponential function. From (40) and (41), we obtain (7) since $\operatorname{Var}\{r(t)\} = \mathbb{E}\{r^2(t)\} - \mathbb{E}^2\{r(t)\}$.

To prove (8), we have

$$\begin{aligned}
f_{r(t)}(r) &\stackrel{(a)}{=} \frac{1}{\sqrt{2D_2t}} f_{\gamma}(\gamma) \\
&\stackrel{(b)}{=} \frac{r}{r_0 \sqrt{\pi D_2t}} \exp\left(-\frac{r^2 + r_0^2}{4D_2t}\right) \sinh\left(\frac{r_0 r}{2D_2t}\right), \quad (42)
\end{aligned}$$

where $f_{\gamma}(\gamma)$ is the PDF of γ . Equality (a) in (42) exploits the fact that γ is a function of $r(t)$ [34, eq. (5)-(16)].

Equality (b) in (42) is obtained from the expression for PDF $f_{\gamma}(\gamma)$ [28, eq. (1.6)] and the relation $I_{1/2}(x) = \sqrt{\frac{2}{\pi x}} \sinh(x)$, where $I_{1/2}(x)$ is the Bessel function of the first kind and order 1/2.

Moreover, since $\frac{r(t)}{\sqrt{2D_2t}}$ follows a noncentral chi distribution, we obtain (9) as [29, eq. (1)]

$$F_{r(t)}(r) = F_{\frac{r(t)}{\sqrt{2D_2t}}}\left(\frac{r}{\sqrt{2D_2t}}\right) = 1 - \mathbf{Q}_{\frac{3}{2}}\left(\lambda, \frac{r}{\sqrt{2D_2t}}\right). \quad (43)$$

APPENDIX B
PROOF OF THEOREM 2

For this proof, we keep in mind that $\hat{h}(r, \tau)$ and $h(t, \tau)$ are two functions of different variables but give the same value h since r is a function of t . Taking the derivative of (1) with respect to r , we obtain (18). From (18), we observe that $\hat{h}'(r, \tau) = 0$ is equivalent to a cubic equation in r , given by $ar^3 + br^2 + cr + d = 0$, with properly defined coefficients a, b, c, d and discriminant $\Delta = 18abcd - 4b^3d + b^2c^2 - 4ac^3 - 27a^2d^2$. From (18), we have $\Delta < 0$ and thus $\hat{h}'(r, \tau) = 0$ has only one real valued solution, denoted by r^* , which corresponds to the maximum value of $\hat{h}(r, \tau)$, denoted by h^* . Then, from (18), we observe that $\hat{h}'(r, \tau) > 0$ for $r < r^*$ and $\hat{h}'(r, \tau) < 0$ for $r > r^*$. Therefore, the equation $\hat{h}(r, \tau) = h$ has two solutions $r_1(h)$ and $r_2(h)$, $r_1(h) < r_2(h)$, when $h < h^*$, and has only one solution r^* when $h = h^* = \hat{h}(r^*, \tau)$. Finally, we derive (17) by exploiting [34, eq. (5)-(16)] for the PDF of functions of random variables. Moreover, for $h = h^*$, $\hat{h}'(r, \tau) = 0$ so $f_{h(t, \tau)}(h) = \frac{f_{r(t)}(r^*)}{\hat{h}'(r^*, \tau)} \rightarrow \infty$.

APPENDIX C
PROOF OF LEMMA 2

To prove Lemma 2, we need to prove that $\operatorname{erf}(\zeta_i(\xi, \alpha_i)) - \operatorname{erf}(\frac{\xi - \eta}{\sqrt{2\eta}})$ is convex in ξ . $\operatorname{erf}(\cdot)$ is a convex and non-decreasing function for negative arguments and a concave and non-decreasing function for positive arguments. For $\eta < \xi < \mu_{i,1}$, we have $\zeta_i(\xi, \alpha_i) < 0$ and $\frac{\xi - \eta}{\sqrt{2\eta}} > 0$. Moreover, $\zeta_i(\xi, \alpha_i)$ and $\frac{\xi - \eta}{\sqrt{2\eta}}$ are affine functions of ξ . Then, $\operatorname{erf}(\zeta_i(\xi, \alpha_i))$ is a convex and non-decreasing function of an affine function and thus is convex in ξ [32, eq. (3.10)]. $\operatorname{erf}(\frac{\xi - \eta}{\sqrt{2\eta}})$ is a concave and non-decreasing function of an affine function and thus is concave in ξ [32, eq. (3.10)]. Therefore, $\operatorname{erf}(\zeta_i(\xi, \alpha_i)) - \operatorname{erf}(\frac{\xi - \eta}{\sqrt{2\eta}})$ is convex, which concludes the proof.

APPENDIX D
PROOF OF LEMMA 3

To prove Lemma 3, we need to prove that $\operatorname{erf}(\zeta_i(\xi, \alpha_i))$ is convex in α . First, $\operatorname{erf}(\cdot)$ is a convex and non-decreasing function for negative arguments and $\zeta_i(\xi, \alpha_i) < 0$ for $\xi < \mu_{i,1}$. Second, when $\eta < \xi$, $\zeta_i(\xi, \alpha_i)$ is a convex function in α since its Hessian matrix is positive semi-definite. Then, $\operatorname{erf}(\zeta_i(\xi, \alpha_i))$ is a convex and non-decreasing function of a

convex function, and thus, it is convex in α for $\eta < \xi < \mu_{i,1}$ [32, eq. (3.10)], which concludes the proof.

APPENDIX E PROOF OF LEMMA 4

To prove Lemma 4, we need to prove $\frac{\partial F_{r(t)}(r)}{\partial t} < 0$. Using the Taylor series expansion of the $\sinh(\cdot)$ function in (8), we obtain

$$\begin{aligned} & \frac{\partial F_{r(t)}(r)}{\partial t} \\ &= \frac{\partial}{\partial t} \left(\int_0^r \frac{x}{r_0 \sqrt{\pi D_2 t}} \exp\left(-\frac{x^2 + r_0^2}{4D_2 t}\right) \right. \\ & \quad \times \sum_{n=0}^{\infty} \frac{1}{(2n+1)!} \left(\frac{r_0 x}{2D_2 t}\right)^{2n+1} dx \Big) \\ &= \int_0^r \frac{x}{r_0 \sqrt{\pi D_2 t}} \sum_{n=0}^{\infty} \left[\frac{1}{(2n+1)!} \left(\frac{r_0 x}{2D_2 t}\right)^{2n+1} \right. \\ & \quad \times \frac{\partial}{\partial t} \left(\exp\left(-\frac{x^2 + r_0^2}{4D_2 t}\right) t^{-2n-3/2} \right) \Big] dx \\ &= \int_0^r \frac{x}{r_0 \sqrt{\pi D_2 t}} \sum_{n=0}^{\infty} \left[\frac{1}{(2n+1)!} \left(\frac{r_0 x}{2D_2 t}\right)^{2n+1} \right. \\ & \quad \times \exp\left(-\frac{x^2 + r_0^2}{4D_2 t}\right) t^{-2n-5/2} \\ & \quad \times \left. \left(-2n - 3/2 + \frac{x^2 + r_0^2}{4D_2 t}\right) \right] dx \\ &\leq 0. \end{aligned} \quad (44)$$

REFERENCES

- [1] T. N. Cao *et al.*, "Diffusive mobile MC for controlled-release drug delivery with absorbing receiver," in *Proc. IEEE Int. Conf. Commun.*, Shanghai, China, May 2019, pp. 1–7.
- [2] V. Jamali, A. Ahmadzadeh, W. Wicke, A. Noel, and R. Schober, "Channel modeling for diffusive molecular communication—A tutorial review," *Proc. IEEE*, vol. 107, no. 7, pp. 1256–1301, Jul. 2019.
- [3] H. B. Yilmaz, A. C. Heren, T. Tugcu, and C.-B. Chae, "Three-dimensional channel characteristics for molecular communications with an absorbing receiver," *IEEE Commun. Lett.*, vol. 18, no. 6, pp. 929–932, Jun. 2014.
- [4] N. Farsad, H. B. Yilmaz, A. Eckford, C.-B. Chae, and W. Guo, "A comprehensive survey of recent advancements in molecular communication," *IEEE Commun. Surveys Tuts.*, vol. 18, no. 3, pp. 1887–1919, 3rd Quart., 2016.
- [5] M. Femminella, G. Reali, and A. V. Vasilakos, "A molecular communications model for drug delivery," *IEEE Trans. Nanobiosci.*, vol. 14, no. 8, pp. 935–945, Dec. 2015.
- [6] S. Kadloor, R. S. Adve, and A. W. Eckford, "Molecular communication using Brownian motion with drift," *IEEE Trans. Nanobiosci.*, vol. 3, no. 1, pp. 89–99, Jun. 2012.
- [7] A. Noel, K. C. Cheung, and R. Schober, "Improving receiver performance of diffusive molecular communication with enzymes," *IEEE Trans. Nanobiosci.*, vol. 13, no. 1, pp. 31–43, Mar. 2014.
- [8] U. A. K. Chude-Onokwwo, R. Malekian, B. T. Maharaj, and A. V. Vasilakos, "Molecular communication and nanonetwork for targeted drug delivery: A survey," *IEEE Commun. Surveys Tuts.*, vol. 19, no. 4, pp. 3046–3096, May 2017.
- [9] A. Guney, B. Atakan, and O. B. Akan, "Mobile ad hoc nanonetworks with collision-based molecular communication," *IEEE Trans. Mobile Comput.*, vol. 11, no. 3, pp. 353–366, Mar. 2012.
- [10] T. Nakano *et al.*, "Performance evaluation of leader–follower-based mobile molecular communication networks for target detection applications," *IEEE Trans. Commun.*, vol. 65, no. 2, pp. 663–676, Feb. 2017.
- [11] G. Chang, L. Lin, and H. Yan, "Adaptive detection and ISI mitigation for mobile molecular communication," *IEEE Trans. Nanobiosci.*, vol. 17, no. 1, pp. 21–35, Jan. 2018.
- [12] L. Lin, Q. Wu, F. Liu, and H. Yan, "Mutual information and maximum achievable rate for mobile molecular communication systems," *IEEE Trans. Nanobiosci.*, vol. 17, no. 4, pp. 507–517, Oct. 2018.
- [13] A. Ahmadzadeh, V. Jamali, and R. Schober, "Stochastic channel modeling for diffusive mobile molecular communication systems," *IEEE Trans. Commun.*, vol. 66, no. 12, pp. 6205–6220, Dec. 2018.
- [14] W. Haselmayr, S. M. H. Aejaz, A. T. Asyhari, A. Springer, and W. Guo, "Transposition errors in diffusion-based mobile molecular communication," *IEEE Commun. Lett.*, vol. 21, no. 9, pp. 1973–1976, Sep. 2017.
- [15] N. Varshney, W. Haselmayr, and W. Guo, "On flow-induced diffusive mobile molecular communication: First hitting time and performance analysis," *IEEE Trans. Mol. Biol. Multi-Scale Commun.*, vol. 4, no. 4, pp. 195–207, Dec. 2018.
- [16] N. Varshney, A. K. Jagannatham, and P. K. Varshney, "On diffusive molecular communication with mobile nanomachines," in *Proc. Annu. Conf. Inf. Sci. Syst.*, Princeton, NJ, USA, Mar. 2018, pp. 1–6.
- [17] M. Sefidgar, M. Soltani, K. Raahemifar, H. Bazmara, S. Nayinian, and M. Bazargan, "Effect of tumor shape, size, and tissue transport properties on drug delivery to solid tumors," *J. Biol. Eng.*, vol. 8, no. 12, p. 12, Jun. 2014.
- [18] A. Pluen, P. A. Netti, R. K. Jain, and D. A. Berk, "Diffusion of macromolecules in agarose gels: Comparison of linear and globular configurations," *Biophys. J.*, vol. 77, no. 1, pp. 542–552, Jul. 1999.
- [19] B. K. Lee, Y. H. Yun, and K. Park, "Smart nanoparticles for drug delivery: Boundaries and opportunities," *Chem. Eng. Sci.*, vol. 125, pp. 158–164, Mar. 2015.
- [20] X. Wang *et al.*, "Diffusion of drug delivery nanoparticles into biogels using time-resolved microMRI," *J. Phys. Chem. Lett.*, vol. 5, no. 21, pp. 3825–3830, Oct. 2014.
- [21] K. B. Sutradhar and C. D. Sumi, "Implantable microchip: The futuristic controlled drug delivery system," *Drug Del.*, vol. 23, no. 1, pp. 1–11, Apr. 2014.
- [22] Y. Chahibi, M. Pierobon, and I. F. Akyildiz, "Pharmacokinetic modeling and biodistribution estimation through the molecular communication paradigm," *IEEE Trans. Biomed. Eng.*, vol. 62, no. 10, pp. 2410–2420, Oct. 2015.
- [23] S. Salehi *et al.*, "Releasing rate optimization in a single and multiple transmitter local drug delivery system with limited resources," *Nano Commun. Netw.*, vol. 11, pp. 114–122, Mar. 2017.
- [24] S. Salehi, N. S. Moayedian, S. H. Javanmard, and E. Alarcón, "Lifetime improvement of a multiple transmitter local drug delivery system based on diffusive molecular communication," *IEEE Trans. Nanobiosci.*, vol. 17, no. 3, pp. 352–360, Jul. 2018.
- [25] N. Farsad and A. Goldsmith, "A molecular communication system using acids, bases and hydrogen ions," in *Proc. IEEE Int. Workshop Signal Process. Adv. Wireless Commun.*, Edinburgh, U.K., Jul. 2016, pp. 1–6.
- [26] V. Jamali, N. Farsad, R. Schober, and A. Goldsmith, "Diffusive molecular communications with reactive signaling," in *Proc. IEEE Int. Conf. Commun.*, Kansas City, MO, USA, May 2018, pp. 1–7.
- [27] A. Ahmadzadeh, V. Jamali, A. Noel, and R. Schober, "Diffusive mobile molecular communications over time-variant channels," *IEEE Commun. Lett.*, vol. 21, no. 6, pp. 1265–1268, Jun. 2017.
- [28] K. S. Miller, R. I. Bernstein, and L. Blumenson, "Generalized Rayleigh processes," *Quart. Appl. Math.*, vol. 16, no. 2, pp. 137–145, Jul. 1958.
- [29] G. H. Robertson, "Computation of the noncentral chi-square distribution," *Bell Syst. Tech. J.*, vol. 48, no. 1, pp. 201–207, Jan. 1969.
- [30] Y. Deng, A. Noel, M. Elkhashan, A. Nallanathan, and K. C. Cheung, "Modeling and simulation of molecular communication systems with a reversible adsorption receiver," *IEEE Trans. Mol. Biol. Multi-Scale Commun.*, vol. 1, no. 4, pp. 347–362, Dec. 2015.
- [31] A. P. Prudnikov, Y. A. Brychkov, and O. I. Marichev, *Integrals and Series*, vol. 1. New York, NY, USA: Gordon & Breach, 1986.
- [32] S. Boyd and L. Vandenberghe, *Convex Optimization*. Cambridge, U.K.: Cambridge Univ. Press, 2004.
- [33] D. A. Stephens. (2008). *Math 556 Mathematical Statistics I*. [Online]. Available: <http://www.math.mcgill.ca/dstephens/556/Handouts/Math556-04-Inequalities.pdf>
- [34] A. Papoulis and S. U. Pillai, *Probability, Random Variables and Stochastic Processes*. New York, NY, USA: McGraw-Hill, 2002.
- [35] D. Y. Arifin, L. Y. Lee, and C. Wang, "Mathematical modeling and simulation of drug release from microspheres: Implications to drug delivery systems," *Adv. Drug Del. Rev.*, vol. 58, no. 12, pp. 1274–1325, Sep. 2006.

- [36] S. Fredenberg, M. Wahlgren, M. Reslow, and A. Axelsson, "The mechanisms of drug release in poly(lactic-co-glycolic acid)-based drug delivery systems—A review," *Int. J. Pharmaceutics*, vol. 415, no. 1, pp. 34–52, May 2011.
- [37] J. H. Park, "Moments of the generalized Rayleigh distribution," *Quart. Appl. Math.*, vol. 19, no. 1, pp. 45–49, Apr. 1961.



Trang Ngoc Cao (Student Member, IEEE) received the B.E. degree in electronics and telecommunications from the Posts and Telecommunications Institute of Technology, Vietnam, in 2012, and the M.S. degree in electronics and radio engineering from Kyung Hee University, South Korea, in 2015. She is currently pursuing the Ph.D. degree with the University of Melbourne, Australia. From 2018 to 2019, she was a Visiting Research Scholar with the Friedrich–Alexander University of Erlangen–Nuremberg, Germany. Her research interests are in

communications theory, information theory, and statistical signal processing with a focus on molecular communications. She received several awards, including the Student Travel Grants for attending the IEEE International Conference on Communications in 2019, the Best Poster Award from the Australian Communication Theory Workshop in 2019, and the Diane Lemaire Scholarship from the Melbourne School of Engineering in 2018.



Arman Ahmadzadeh (Student Member, IEEE) received the B.Sc. degree in electrical engineering from the Ferdowsi University of Mashhad, Mashhad, Iran, in 2010, and the M.Sc. degree in communications and multimedia engineering from the Friedrich–Alexander University of Erlangen–Nuremberg, Erlangen, Germany, in 2013, where he is currently pursuing the Ph.D. degree in electrical engineering with the Institute for Digital Communications. His research interests include physical layer molecular communications. He

received several awards, including the Best Paper Award from the IEEE ICC in 2016, the Student Travel Grants for attending the Global Communications Conference in 2017, and was recognized as an Exemplary Reviewer of IEEE COMMUNICATIONS LETTERS in 2016. He served as a member of Technical Program Committees of the Communication Theory Symposium for the IEEE International Conference on Communications (ICC) in 2017 and 2018.



Vahid Jamali (Member, IEEE) received the B.S. and M.S. degrees (Hons.) in electrical engineering from the K. N. Toosi University of Technology, Tehran, Iran, in 2010 and 2012, respectively, and the Ph.D. degree (with Distinction) from the Friedrich–Alexander-University (FAU) of Erlangen–Nürnberg, Erlangen, Germany, in 2019.

In 2017, he was a Visiting Research Scholar with Stanford University, Stanford, CA, USA. He is currently a Postdoctoral Fellow with the Institute for Digital Communication, FAU. His research interests

include wireless and molecular communications, Bayesian inference and learning, and multiuser information theory. He received several awards, including the Best Paper Award from the IEEE International Conference on Communications in 2016, the Best Paper Award from the ACM International Conference on Nanoscale Computing and Communication in 2019, the Best Poster Award from the Australian Communication Theory Workshop in 2019, the Exemplary Reviewer Certificates from IEEE COMMUNICATIONS LETTERS in 2014 and the IEEE TRANSACTIONS ON COMMUNICATIONS in 2017 and 2018, the Doctoral Scholarship from the German Academic Exchange Service in 2017, and the Goldener Igel Publication Award from the Telecommunications Laboratory, FAU, in 2018. He has served as a member of the technical program committees for several IEEE conferences. He is currently an Associate Editor of IEEE COMMUNICATIONS LETTERS and the IEEE OPEN JOURNAL OF THE COMMUNICATIONS SOCIETY.



Wayan Wicke (Student Member, IEEE) was born in Nuremberg, Germany, in 1991. He received the B.Sc. and M.Sc. degrees in electrical engineering from the Friedrich–Alexander University Erlangen–Nürnberg, Erlangen, Germany, in 2014 and 2017, respectively, where he is currently pursuing the Ph.D. degree. His research interests include statistical signal processing and digital communications with a focus on molecular communication.



Phee Lep Yeoh (Member, IEEE) received the B.E. degree (University Medal) and the Ph.D. degree from the University of Sydney (USYD), Australia, in 2004 and 2012, respectively.

From 2005 to 2008, he was a Wireless Technology Specialist with Telstra, Australia. From 2012 to 2016, he was a Lecturer and a Research Fellow of wireless communications with the University of Melbourne, Australia. Since 2016, he has been a Senior Lecturer with the School of Electrical and Information Engineering, USYD. His current research interests include secure wireless communications, ultrareliable and low-latency communications, and multiscale molecular communications. He is a recipient of the 2020 USYD Robinson Fellowship, the 2018 Alexander von Humboldt Research Fellowship for Experienced Researchers, and the 2014 Australian Research Council Discovery Early Career Researcher Award. He has received Best Paper Awards at IEEE ICC 2014 and IEEE VTC-Spring 2013, and Best Student Paper Awards with his supervised students at the 2013 and 2019 Australian Communications Theory Workshop.



Jamie Evans (Senior Member, IEEE) was born in Newcastle, Australia, in 1970. He received the B.S. degree (University Medal) in physics and the B.E. degree (University Medal) in computer engineering from the University of Newcastle in 1992 and 1993, respectively, and the M.S. and Ph.D. degrees in electrical engineering from the University of Melbourne, Australia, in 1996 and 1998, respectively, and was awarded the Chancellor's Prize for Excellence for his Ph.D. thesis. From March 1998 to June 1999, he was a Visiting Researcher with the Department

of Electrical Engineering and Computer Science, University of California, Berkeley. Since returning to Australia in July 1999, he has held academic positions with the University of Sydney, the University of Melbourne, and Monash University. He is currently a Professor and the Deputy Dean of the Melbourne School of Engineering, University of Melbourne. His research interests are in communications theory, information theory, and statistical signal processing with a focus on wireless communications networks.



Robert Schober (Fellow, IEEE) received the Diplom (Univ.) and the Ph.D. degrees in electrical engineering from the Friedrich–Alexander University of Erlangen–Nuremberg (FAU), Germany, in 1997 and 2000, respectively.

From 2002 to 2011, he was a Professor and Canada Research Chair with the University of British Columbia (UBC), Vancouver, Canada. Since January 2012, he has been an Alexander von Humboldt Professor and Chair of Digital Communication with FAU. His research interests

fall into the broad areas of communication theory, wireless communications, and statistical signal processing. He received several awards for his work, including the 2002 Heinz Maier Leibnitz Award of the German Science Foundation (DFG), the 2004 Innovations Award of the Vodafone Foundation for Research in Mobile Communications, the 2006 UBC Killam Research Prize, the 2007 Wilhelm Friedrich Bessel Research Award of the Alexander von Humboldt Foundation, the 2008 Charles McDowell Award for Excellence in Research from UBC, the 2011 Alexander von Humboldt Professorship, the 2012 NSERC E.W.R. Stacie Fellowship, and the 2017 Wireless Communications Recognition Award by the IEEE Wireless Communications Technical Committee. Since 2017, he has been listed as a Highly Cited Researcher by the Web of Science. From 2012 to 2015, he served as the Editor-in-Chief for the IEEE TRANSACTIONS ON COMMUNICATIONS. He currently serves as an Editorial Board Member of the PROCEEDINGS OF THE IEEE and as VP Publications for the IEEE Communications Society. He is a fellow of the Canadian Academy of Engineering and the Engineering Institute of Canada.